

Large-scale dam removal on the Elwha River, Washington, USA: Coastal geomorphic change



Guy Gelfenbaum^{a,*}, Andrew W. Stevens^a, Ian Miller^b, Jonathan A. Warrick^a, Andrea S. Ogston^c, Emily Eidam^c

^a U.S. Geological Survey, 400 Natural Bridges Drive, Santa Cruz, CA 95060, USA

^b Washington Sea Grant, Olympic Peninsula Field Office, 1502 E. Lauridsen Blvd. #82, Port Angeles, WA 98362, USA

^c University of Washington, School of Oceanography, Box 357940, Seattle, WA 98195, USA

ARTICLE INFO

Article history:

Received 30 June 2014

Received in revised form 29 December 2014

Accepted 5 January 2015

Available online 9 January 2015

Keywords:

Elwha River

Dam removal

Delta

Coastal change

Delft3D model

Sediment dispersal

ABSTRACT

Two dams on the Elwha River, Washington State, USA trapped over 20 million m³ of mud, sand, and gravel since 1927, reducing downstream sediment fluxes and contributing to erosion of the river's coastal delta. The removal of the Elwha and Glines Canyon dams, initiated in September 2011, induced massive increases in river sediment supply and provided an unprecedented opportunity to examine the geomorphic response of a coastal delta to these increases. Detailed measurements of beach topography and nearshore bathymetry show that ~2.5 million m³ of sediment was deposited during the first two years of dam removal, which is ~100 times greater than deposition rates measured prior to dam removal. The majority of the deposit was located in the intertidal and shallow subtidal region immediately offshore of the river mouth and was composed of sand and gravel. Additional areas of deposition include a secondary sandy deposit to the east of the river mouth and a muddy deposit west of the mouth. A comparison with fluvial sediment fluxes suggests that ~70% of the sand and gravel and ~6% of the mud supplied by the river was found in the survey area (within about 2 km of the mouth). A hydrodynamic and sediment transport model, validated with in-situ measurements, shows that tidal currents interacting with the larger relict submarine delta help disperse fine sediment large distances east and west of the river mouth. The model also suggests that waves and currents erode the primary deposit located near the river mouth and transport sandy sediment eastward to form the secondary deposit. Though most of the substrate of the larger relict submarine delta was unchanged during the first two years of dam removal, portions of the seafloor close to the river mouth became finer, modifying habitats for biological communities. These results show that river restoration, like natural changes in river sediment supply, can result in rapid and substantial coastal geomorphological responses.

Published by Elsevier B.V.

1. Introduction

River mouths are conduits for the transfer of terrestrial sediments to coastal and marine environments, where they form habitats that support biological communities and protect adjacent development and infrastructure from flooding and erosion. Upon reaching the river mouth, sediments are typically stored, at least temporarily, in deltas (Wright and Coleman, 1973). Some fraction of the fine sediments (silts and clays) may be stored subaerially in delta floodplains by overbank flows but the majority of fines will be deposited in subaqueous portions of the delta (Wright, 1977) or dispersed farther offshore in buoyant plumes (e.g., Geyer et al., 2000). Coarser sediments (sands and gravels) will be deposited proximally in delta fronts and sediment size generally will fine with distance from the river mouth to the pro-deltas (Wright and Coleman, 1973; Wright, 1977).

* Corresponding author. Tel: +1 831 460 7417.

E-mail addresses: ggelfenbaum@usgs.gov (G. Gelfenbaum), astevens@usgs.gov (A.W. Stevens), immiller@uw.edu (I. Miller), jwarrick@usgs.gov (J.A. Warrick), ogston@ocean.washington.edu (A.S. Ogston), efe@uw.edu (E. Eidam).

River deltas are known to adopt different morphologies depending on varying hydrologic and hydrodynamic processes. Based on field observations from around the world, delta morphologies have been classified according to the relative importance of tides, waves, and river discharge (Galloway, 1975; Wright, 1977). The classification has been extended to include the effect of sediment grain size on morphology (Orton and Reading, 1993), and recently Geleynse et al. (2011) demonstrated the effect of antecedent stratigraphy on delta evolution via a process-based sediment transport model.

Not as well understood is the role that deltas play in transferring sediment to adjacent beaches and nearshore zones. Coarse sediments may be temporarily deposited in an active prograding delta front, which can store sediment delivered from the river and transfer it to the coast or offshore at a later time through erosion and transport processes (Hicks and Inman, 1987; Barnard and Warrick, 2010). The amount of sediment stored in a delta depends on the combination of several interacting factors, including wave and current energy, sea level, accommodation space, and sediment supply (Wright, 1977). Goodbred and Kuehl (1999) estimated that over hundreds to thousands

of years about 30–40% of the sediment load of the Ganges–Brahmaputra River system was stored in its delta while the remaining load was deposited in the floodplain or offshore. Their analysis did not resolve questions of short-term (seasonal or storm event) storage in the delta and transfer to the coast or offshore.

Perturbations from natural or anthropogenic forces can change the sediment budget and morphology of a delta. For example, Kuenzi et al. (1979) described 7 km of progradation of the Samala River delta following a large increase in sediment supply associated with the eruption of the Santa Maria volcano in southwestern Guatemala. Kaminsky et al. (2010) and Gelfenbaum and Kaminsky (2010) documented changes to the Columbia River delta and adjacent shorelines in the northwest United States as a result of large jetties constructed at the river's mouth modifying the local sediment supply. Dams may reduce sediment supply to the coast and alter the dynamic equilibrium of the delta, prompting a change in the morphology of the delta or adjacent coastal zone as has been suggested for the California coast (Willis and Griggs, 2003), the Nile River delta on the Egyptian coast (Smith and Abdel-Kader, 1988), and the Ebro River delta on the northeastern Spanish coast (Jimenez and Sanchez-Arcilla, 1993; Sanchez-Arcilla et al., 1998). In the latter two cases, reduced sediment supply was documented to alter delta morphology, littoral sediment budgets, and coastal habitats (Fatorić and Chelleri, 2012). For example, reduced sediment loads changed the Ebro delta from an intermediate river–wave-dominated system to a purely wave-dominated system (Jimenez and Sanchez-Arcilla, 1993).

In this paper we examine the Elwha River in Washington State in the U.S. Pacific Northwest, where two dams built in the early 1900s trapped ~21 million m³ of sediment, reducing sediment loads to the coast (Warrick et al., 2009a; Draut et al., 2011; Miller et al., 2011). Shoreline erosion and a coarsening of the beach low-tide terrace are hypothesized to have resulted from sediment supply deficiencies to the coast after the dams were built (Warrick et al., 2009a). Removal of the two dams on the Elwha River, which began in September 2011, provides a unique opportunity to examine a complex system adjustment to a major sediment pulse by quantifying the landscape response of a coastal delta to dam removal.

The goal of this paper is to document the changes to the Elwha River delta during the first two years of dam removal and evaluate the causes of observed changes. In this paper, we (i) describe the accumulation of sediment on the Elwha delta by comparing detailed digital elevation models (DEMs) made from repeated surveys of beach topography and nearshore bathymetry; (ii) document the beach and seafloor grain size changes throughout this coastal system, (iii) calculate a sediment budget from sediment volume and grain size changes in the delta relative to the delivery of sediment from the river to address where sediment goes after it reaches the coast; and (iv) use a process-based hydrodynamics and sediment transport model, validated against field data, in order to explain the measured patterns of sediment accumulation on the delta after the sediment supply increased.

This paper is one of five addressing the geomorphic responses of the Elwha River system during the first two years of dam removal. Companion papers describe: (i) geomorphic changes in the reservoirs (Randle et al., 2015), (ii) sediment transport in the river (Magirl et al., 2015), (iii) geomorphic response of the Elwha river and floodplain (East et al., 2015), and (iv) a synthesis of the sediment budget (Warrick et al., 2015).

2. Regional setting

2.1. Watershed, river, dams, sediment impoundment

The Elwha River drains the largest north-facing watershed of the Olympic Mountains in Washington State, USA, with 83% of the 831-km² watershed lying in the Olympic National Park (Fig. 1) (Duda et al., 2011). The river flows north, entering the Strait of Juan de Fuca

just west of the city of Port Angeles, WA, and on the western side of a nearly symmetrical subaerial delta (Fig. 1B and C). The subaerial delta is offset from the larger, relict submarine delta. In this paper we will also use the term active delta to describe the relatively new depositional zone near the mouth of the river and the inner delta to describe the shallow parts of the larger submarine delta. Discharge from the river averages ~40 m³/s (USGS gauge 12046260; Fig. 1B) and varies seasonally with higher flows associated with snowmelt in spring and rainfall events in early winter. The lowest discharge typically occurs in late summer (Duda et al., 2011; Magirl et al., 2011). Peak discharge of around 400 m³/s occurs every two years on average, and in December 2007 discharge reached 1000 m³/s, which was estimated to be a 40-year flood event (Draut et al., 2011).

The river drains metasedimentary rocks in steep, landslide-prone terrain in the upper basin and traverses glacial bluffs of till and outwash in the lower floodplain (Warrick et al., 2009a; Draut et al., 2011). Sediments of all sizes are available to the river. Because of multiple large channels divided by vegetated bars, and large numbers of avulsions, Draut et al. (2011) described the lower river as anabranching. Analysis of historical aerial photographs from 1939 to present shows that the river mouth has not occupied a position near the center of the subaerial delta in at least the past 75 years (Draut et al., 2011). At various times from the 1950s to the present, small earthen or rock dikes were constructed along both sides of the lower river to prevent flooding of nearby homes and roads. Owing to a reduction in sediment supply from damming, much of the lower river-bed had become armored with cobbles (Draut et al., 2011).

Two large concrete dams were built on the river about 100 years ago to generate electricity for local use; the downstream Elwha Dam was completed in 1913 and the upstream Glines Canyon Dam was completed in 1927. Located at river kilometer 7.9 above the mouth, the Elwha Dam was 32 m high and created Lake Aldwell. At river kilometer 21.6, the 64-m high Glines Canyon Dam created Lake Mills (Fig. 1). The dams on the Elwha River caused sediment transport competency to fall as the river approached Lake Mills and Lake Aldwell. Large deltas grew into the upstream end of each reservoir, trapping all coarse sediment and most of the fine sediment supplied from the river (Curran et al., 2009; Czuba et al., 2011). The Lake Mills delta trapped ~16.1 million m³ of sediment by 2010 (Gilbert and Link, 1995; Bountry et al., 2010; Randle et al., 2015). Sediment stored in Lake Mills was composed of ~44% silt and clay, and 56% sand, cobbles and boulders (Gilbert and Link, 1995; Randle et al., 2015). A few kilometers downstream, the Lake Aldwell reservoir trapped ~4.9 million m³ of sediment by 2010, with ~53% silt and clay and 47% sand, gravel, and cobbles (Randle et al., 2015).

Based on the long-term accumulation of sediment in the reservoirs, the average sediment load of the river upstream of the dams is estimated to be 240,000 m³/y ± 60 m³/y (Magirl et al., 2015). This is consistent with the total sediment load calculated from field measurements of suspended- and bedload transport by Curran et al. (2009).

2.2. Dam removal

In 1992, the U.S. Congress passed the Elwha River Ecosystem and Fisheries Restoration Act (PL102-485), and removal of both dams began on 17 September 2011. To limit the potential negative effects of high sediment concentrations from dam removal activities on fish health and spawning and on the operation of a downstream water treatment plant, dam removal was phased over 2–3 years. Lake Aldwell was drained, and the lower Elwha Dam was completely removed by April 2012, approximately 7 months after dam removal initiation (Randle et al., 2015). Lake Mills was fully drained by October 2012, although the final removal of Glines Canyon Dam did not occur until the summer of 2014, a year after the 2-year interval of time studied here. This restoration project is the largest dam decommissioning project in

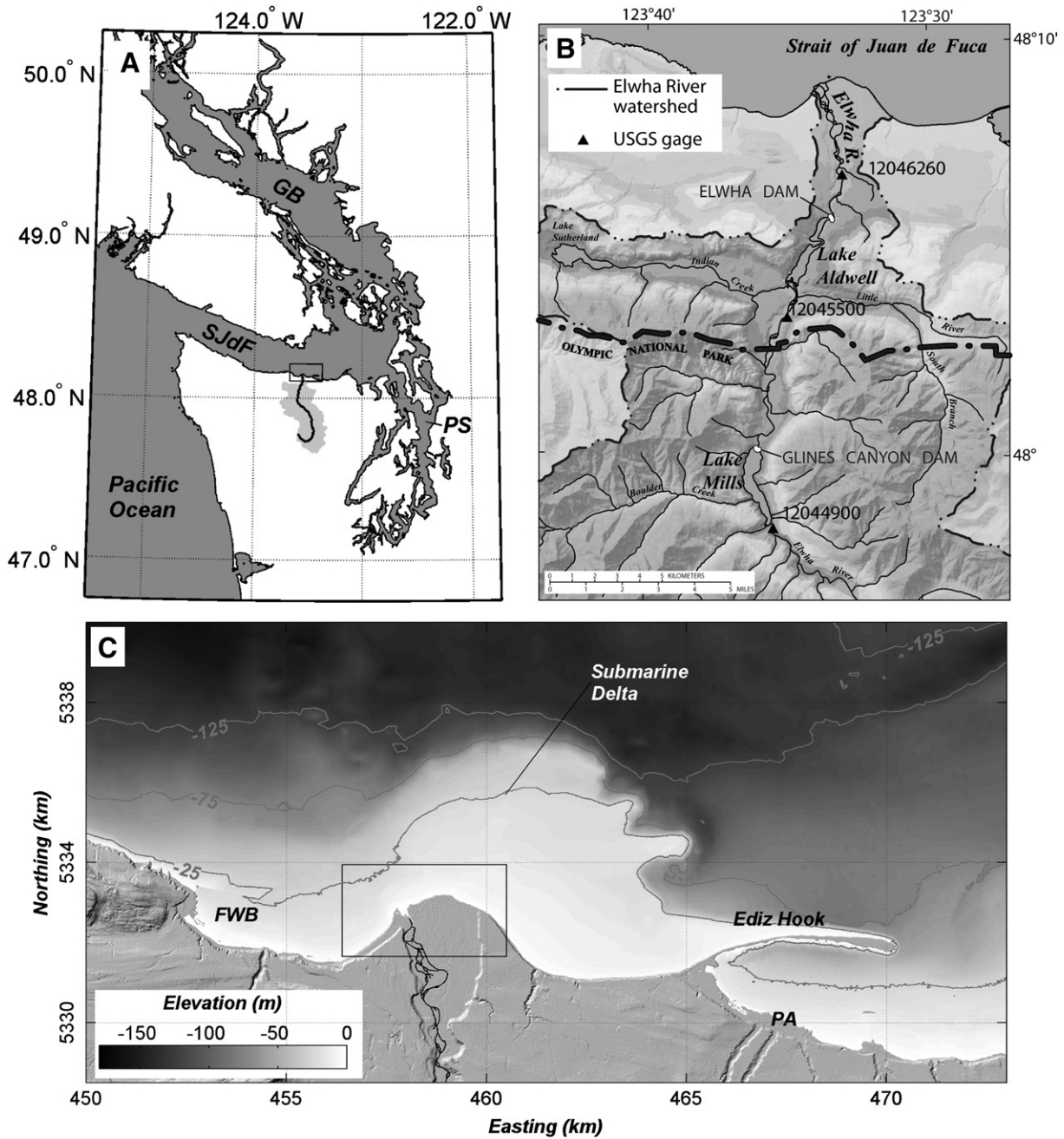


Fig. 1. Location map of study area. (A) The Salish Sea comprised of (GB) Georgia Basin, Strait of Juan de Fuca (SjDf), and Puget Sound (PS). (B) The Elwha watershed showing the former dam locations and reservoirs, and the locations of USGS river gaging stations. (C) The Elwha delta and nearshore. FWB is Freshwater Bay, and PA is Port Angeles. Box over delta in the lower panel is area enlarged in Fig. 3 and other figures of the inner delta.

the U.S. to date in terms of stored sediment and in terms of the size of the hydroelectric projects removed (Duda et al., 2011).

2.3. Large signal, fast response

The Elwha River has a steep gradient, dropping 1400 m from its source to sea level at the delta in only about 70 km. The steepness of the drainage and proximity of the Elwha River dams to the coast was expected to result in a relatively rapid transport of reservoir sediment to the coast during and following dam removal (Gelfenbaum et al., 2011; East et al., 2015). In addition, the quantity of sediment transported to the coast was expected to be easily detectable above the resolution of topographic and bathymetric surveys and easily discernable above the background seasonal and interannual morphology change. The

likelihood of a rapid and easily measurable response to dam removal makes Elwha River restoration ideally suited to comprehensive monitoring and provides a unique opportunity to better understand how changes in sediment supply effect delta geomorphology.

Within a few months after dam removal began, sediment load in the river downstream of Elwha Dam increased measurably (Warrick et al., 2012; Fig. 2). Spikes in suspended-sediment concentration measured at USGS Station 12046260 (Fig. 1B) resulted from small flood events in late 2011 and early in 2012, as well as from relocating temporary earthen coffer dams from one side of the river channel to the other as Elwha Dam was being lowered. In the two years since dam removal started in September 2011, there was ~8.2 million tonnes of cumulative sediment discharge measured in the Elwha River (Fig. 2; Magirl et al., 2015), or 5.9 million m³ of sediment assuming an average bulk density

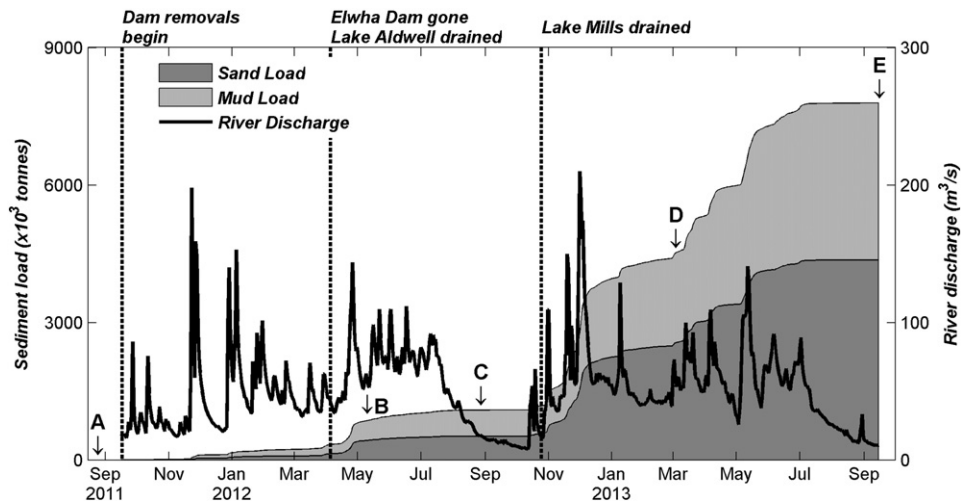


Fig. 2. Time series of Elwha River discharge (thick black line) and cumulative sediment load (shaded curves) measured at USGS gauge 12046260. The location of the river gauge is shown in Fig. 1. Arrows denote times when beach topography and nearshore bathymetry surveys were performed.

of 1.4 tonnes/m³ for reservoir sediments (Magirl et al., 2015). This sediment load was roughly 40% silt and clay by weight and was punctuated by rapid fluxes during higher river flows and immediately following dam deconstruction activities (Fig. 2; Magirl et al., 2015).

2.4. Coastal processes

2.4.1. Currents and waves

Currents in the Strait of Juan de Fuca are predominantly driven by tides, augmented by density-driven gradients resulting from freshwater input from large rivers in Puget Sound and Georgia Basin (Foreman et al., 2004; Sutherland et al., 2011). Tides are mixed, semidiurnal with a mean tidal range of 1.4 m and a spring tide range of 2.2 m. Locally, off the Elwha delta, tidal constituents account for over 84% of the total variance in depth-averaged currents, with the M2 semidiurnal harmonic dominant (Warrick and Stevens, 2011). Current meter observations (Warrick et al., 2011; Eidam et al., in preparation) and numerical model simulations (Gelfenbaum et al., 2009) show tidal currents interacting with the Elwha delta to induce transient eddies in the instantaneous flow as well as large coherent residual currents. On the west side of the delta, tidal residuals flow toward the northeast; whereas on the east side of the delta, the tidal residuals flow toward the northwest. This complex pattern of currents has a strong influence on the dispersal of sediment and on the position of the buoyant plume that comes from the Elwha River (Gelfenbaum et al., 2009; Warrick and Stevens, 2011).

Waves near the Elwha delta originate predominantly from the northwest, propagating as swell into the Strait from the Pacific Ocean. Warrick et al. (2009a) measured waves on the Elwha delta from January to May 2006 and found that waves came from the northwest 91% of the time and from the northeast only 9% of the time. Wave energy can be divided into predominately longer period swell from the northwest and shorter period wind waves from the northeast and the northwest. Wave energy attenuates as it propagates through the Strait and approaches the delta, with wave heights decreasing on average 20–30% between the Strait entrance and the delta (Gelfenbaum et al., 2009; Warrick et al., 2011). During the time period reported by Warrick et al. (2009a), wave heights on the delta only occasionally exceeded 1 m and on average were <0.5 m.

2.4.2. Beach morphology, substrate, and littoral transport

Foreshore beaches on both sides of the Elwha River delta are composed of mixed sand and cobble. Beaches adjacent to the river mouth are steep, with mean gradients around 0.1 to 0.17 (Warrick et al.,

2009a) and are considered reflective per the classification of Wright and Short (1984). East of the river mouth, beaches are erosive, berm elevations average 3.9 m above mean lower low water (MLLW), and at elevations below approximately 0.5 m MLLW there is a wide, nearly flat low-tide terrace composed of large cobbles. Warrick et al. (2011) suggested that this terrace is a coarse lag deposit formed as the foreshore eroded landward. Miller et al. (2011) found very low mean transport rates in the coarse clasts on this low-tide platform. West of the river mouth, beach berm heights average 4.9 m above MLLW (higher than on the east side), there is no low-tide platform, and the beaches are stable and not eroding.

The dominance of wave energy from the northwest drives littoral transport to the east in the drift cell that includes the Elwha delta (Galster and Schwartz, 1990). Locally, however, the shape of the delta modifies littoral drift directions and rates. Given the steep beaches around the Elwha delta, waves tend to break directly on the beach in a shore break, limiting the width of the surf zone and increasing the importance of swash processes on littoral transport. On the west side of the subaerial delta, the alongshore transport rates are relatively small (Miller et al., 2011) and the shoreline position is stable (Warrick et al., 2009a) owing to the generally shore-normal direction of wave incidence. In contrast, waves approach the central and east sides of the subaerial delta from an oblique angle, resulting in greater alongshore transport rates (Miller and Warrick, 2012). Radio tags implanted into beach cobbles by Miller et al. (2011) measured small bidirectional transport on the west side of the delta, while on the east side of the delta they measured much more rapid unidirectional transport to the east, with net cobble velocities exceeding 100 m/d under high-energy wave conditions.

3. Methods

3.1. Nearshore bathymetry and beach topography

Repeated surveys of nearshore bathymetry and beach topography were performed annually from 2009 to 2011 to assess pre-dam removal background conditions and biannually from 2011 to 2013 to assess effects of dam removal. Surveys were conducted during spring tides with nearshore bathymetric measurements made during high tide, and topographic measurements collected during low tide to maximize overlapping data between the two survey platforms. Nearshore bathymetry data were collected using personal watercraft equipped with single-beam sonar and differential GPS operating in real-time kinematic (RTK) mode. Raw bathymetric data were processed and

corrected for the local speed of sound using sound velocity profiles collected during each survey. Topographic surveys were conducted on foot with RTK-GPS equipment mounted on backpacks. Geodetic control was established using a shore-based GPS base station placed on one of several pre-existing benchmarks (Fig. 3). The GPS base stations were programmed with coordinates relative to the NAD83 (CORS96) datum. Elevations in the North American Vertical Datum of 1988 (NAVD88) were computed using the National Geodetic Survey GEOID09 geoid model. Zero elevation in the NAVD88 vertical datum is approximately 13 cm higher than mean lower low water recorded at NOAA Tide Station 9444090 in Port Angeles. We define the shoreline following Warrick et al. (2009a) as the mean high water (MHW) contour, where MHW is 1.98 m above MLLW and 1.86 m above NAVD88.

Bathymetric and topographic measurements were collected primarily along a series of cross-shore transects at roughly 30 m alongshore intervals (Fig. 3) and extend from roughly –14 m water depth to just landward of the foreshore berm at about +5 m elevation. Additional data between transects were collected to better characterize the morphologic variability within the survey area. Digital elevation models (DEMs) were constructed for each survey from all available data using linear, Delaunay interpolation with either 5- or 1-m resolution.

An error analysis was performed to quantify the uncertainty in raw elevation data and resulting DEMs for use in a sediment budget. Errors in the raw elevation data include systematic and random components and are derived from drift in the GPS solution (Sallenger et al., 2003; Ruggiero et al., 2005), surveying equipment set-up and measurement, and uncertainty in speed of sound estimates for the bathymetric data. We calculated a mean systematic within-survey bias of 0.026 m and a mean random uncertainty of 0.036 m from 33 replicate transects collected during bathymetric surveys between August 2011 and September 2013 (Table 1). Errors arising from the gridding method used to create the DEM were estimated using a cross-validation technique (Davis, 2002). Based on removing 1000 randomly selected points, one at a time for each DEM, this procedure suggests that no bias is introduced into the DEMs during the grid interpolation process, and that the mean standard deviation of the grid error is 0.086 m (Table 1). Combining the

estimated errors from both the gridding and the raw elevation data provides a total uncertainty for each DEM (σ_{total}) of 0.13 m.

Elevation uncertainty associated with differencing two DEMs to derive volume change are calculated by summing the sum of the systematic bias components with the sum in quadrature of the random uncertainties estimated from analysis of replicate transects and the grid cross validation described above. We assume that within- and between-survey uncertainties are equivalent. Total elevation uncertainty for the difference between two DEMs is therefore estimated to be ± 0.20 m. Elevation change estimates between surveys <0.2 m are therefore considered unreliable and are labeled as ‘Not Detectable’ (N.D.) in the volume change maps. The uncertainty associated with estimating the volume of sediment from differencing two DEMs is calculated by treating the random and systematic errors separately. The volume uncertainty is calculated by multiplying the survey area by the systematic uncertainty and adding the random component in quadrature (Table 2). Additional details of the uncertainty analysis are provided in the supplemental section of this paper.

3.2. Beach and seafloor substrate characterization

As a result of the morphologic complexity and wide range of sediment sizes within the study area, a variety of techniques were employed to characterize beach and seafloor substrate changes during dam removal. Van Veen grab samples were collected in the shallow subtidal (<15 m) and by hand from the beach at sites across the new sediment deposit near to the river mouth. Approximately 500 g of sediment from each sampling site was analyzed for grain size. Samples were homogenized, split, and then run through a Coulter counter and sieves, providing grain size distributions from 0.0001 to 16 mm. Sampling occurred 28–30 August 2012 at 57 locations, 4–7 March 2013 at 52 locations, and again 16–19 September 2013 at 83 locations. Farther offshore (>15 m depth), Shipek grab samples were obtained from the *R/V Barnes* across the broad subaqueous delta. Silts and clays ($<63 \mu$) were separated from sands and gravels by wet-sieving with a dilute dispersant and then analyzed in a Micromeritics Sedigraph particle size

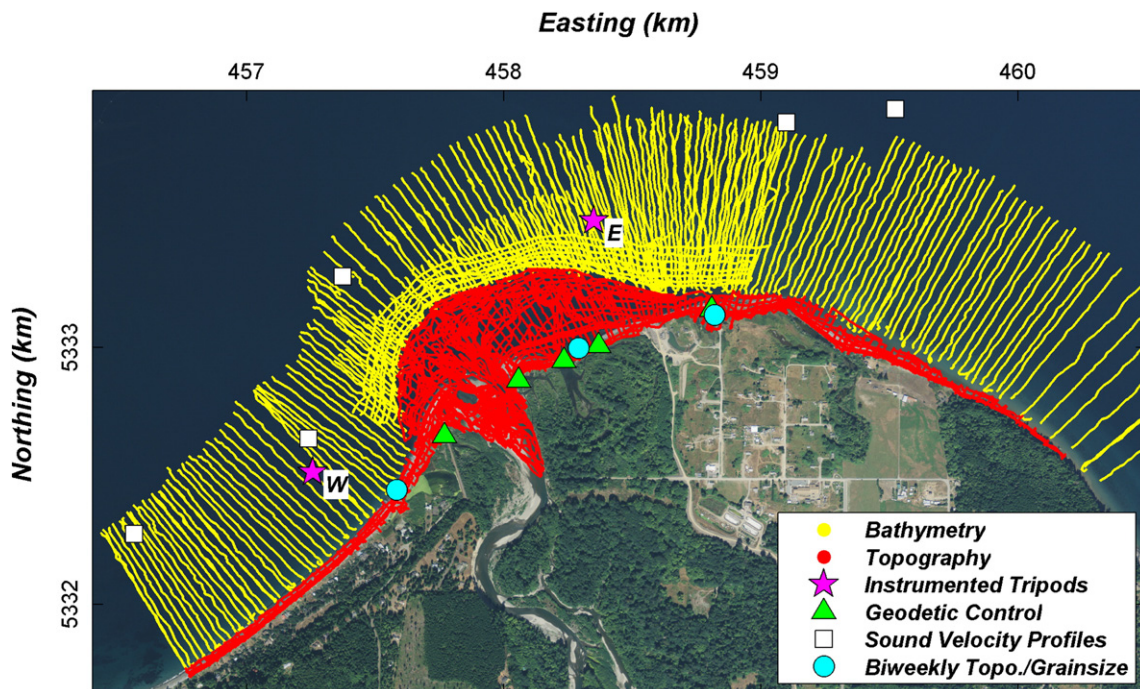


Fig. 3. Map showing locations of beach topographic and nearshore bathymetric data from the September 2013 survey. Also shown are locations of instrumented tripods E and W, geodetic control monuments for GPS base stations (green triangles), sound velocity profiles (white squares) used in speed of sound corrections to bathymetric soundings, and biweekly beach topography and grain size profiles (blue circles).

Table 1Elevation uncertainty estimates; σ represents one standard deviation; σ_{drift} is uncertainty resulting from GPS drift.

Survey	GPS drift	Replicate line analysis			Grid cross validation		Total uncertainty ^a
	σ_{bias} (m)	# of lines	σ_{bias} (m)	σ_{random} (m)	# of points	σ_{random} (m)	σ_{total} (m)
Average	0.01	33	0.026	0.036	1000	0.086	0.13

^a Total uncertainty for each DEM ($\sigma_{\text{total}} = 0.01 + 0.026 + (\text{sqrt}(0.036^2 + 0.086^2)) = 0.13$ m.

analyzer. Sands and gravels were dried and sieved. Grab samples that yielded < 50 g of sediment were omitted from analysis and are classified as ‘no sample’.

The mixed sand, gravel, and cobbles of the beach and intertidal zone of the Elwha River delta were difficult to characterize with standard laboratory techniques, so high-resolution photos of the beach were collected approximately biweekly from September 2011 to 2013 at every 0.25-m elevation interval between 1.0 and 4.0 m MLLW at four cross-shore transects. The digital camera was hand held approximately 0.5 to 1.0 m above the bed, providing images covering an area of between 0.1 and 0.8 m². Each photo was analyzed using an automated digital grain size algorithm (Warrick et al., 2009b) and was converted from pixel to mm units using a ground scale included in each photo. Photos with excessive woody debris or shading were discarded.

Changes in the shallow subtidal substrate associated with dam removal were also characterized from repeated mapping of acoustic backscatter of the seafloor (Finlayson et al., 2011). Surveys conducted from the *R/V Parke Snavelly* using a SWATHPlus interferometric sidescan sonar provided detailed swath bathymetry and acoustic backscatter data to water depths of ~20 m. Mapping was conducted in February 2010 prior to the start of dam removal and again in March 2013, approximately one year after the lower Elwha Dam was completely removed.

3.3. Coastal processes – tripods

Data from two instrumented tripods deployed in 10-m water depth on the east and west side of the river mouth (Fig. 3) help characterize waves and currents around the delta and validate a numerical model of hydrodynamics and sediment transport. Both tripods were equipped with an upward-looking 1200 kHz acoustic Doppler current profiler (ADCP), pressure sensors, and digital cameras and strobes pointing at the seafloor under the tripod. Current velocity profiles were recorded at 5-min intervals from 1.9 m above the bottom to the surface with a vertical resolution of 0.25 m. Wave bursts were recorded for 20 min at 2-h intervals with a sample rate of 2 Hz. Tripods E and W were deployed prior to dam removal on 15 December 2010 and 13 March 2011, respectively. Both tripods recorded data nearly continuously through the first two years of dam removal, with the exceptions of a few gaps for instrument service or repair.

3.4. Numerical model of hydrodynamics and sediment transport

Hydrodynamic and sediment transport modeling was carried out with the process-based model Delft3D (Lesser et al., 2004) to help

understand the processes responsible for sediment dispersal patterns observed in field measurements. The Delft3D model solves the nonlinear, time-dependent, shallow water continuity and momentum equations to simulate water motion from tides, waves, wind, and buoyancy effects. The lower resolution Salish Sea model (see Salish Sea and nested model descriptions in Supplemental documents) was forced at a single open boundary at the entrance to the Strait of Juan de Fuca with harmonic tidal constituents. Fresh water from several rivers in the Salish Sea was included.

Additionally, waves were simulated using the third-generation SWAN wave model, which simulates wave propagation in time and space by solving the spectral action balance equation (Booij et al., 1999; Elias et al., 2012). The wave model was forced at a single open boundary on the seaward end with a time-series of wave parameters obtained from Wavewatch III model output to simulate swell entering the model domain from the Pacific Ocean. Wave output is used in the flow model to simulate enhanced bed stresses due to waves (Soulsby et al., 1993) and wave-driven currents (Walstra et al., 2000) (see SWAN model development in Supplemental documents).

A high-resolution, nested grid is used to compute hydrodynamics and sediment transport in the vicinity of the Elwha River delta. The Elwha model grid has a minimum grid size of ~18 m² near the river mouth. Nine vertical water layers are used to simulate 3D effects, in particular buoyancy-controlled flows, within the model domain. The model bottom boundary includes beach topography and nearshore bathymetry data collected by this study prior to dam removal (September 2011) as well as high-resolution swath bathymetry collected in 2010 (Finlayson et al., 2011).

Discharge from the Elwha River provides a boundary condition into the model domain using measurements of river discharge at USGS Station 12046260 and sediment concentration from Magirl et al. (2015) (Fig. 1). Two sediment fractions are simulated in the model, sand (0.2 mm) and mud ($w_s = 2.5 \times 10^{-3}$ cm/s), using sediment concentrations as measured by Magirl et al. (2015); gravel was not modeled.

Sediment transport for noncohesive and cohesive particles is computed in the Delft3D model simulations (Lesser et al., 2004). To account for the coarse, armored nature of the seafloor prior to dam removal, the bed schematization includes a single, well-mixed layer with no sediment on the bed initially available for erosion. If sediment is deposited during a simulation, then that newly deposited sediment can be resuspended and transported.

The hydrodynamic and sediment transport models were run for the time period between 01 April 2012 and 20 May 2012 to simulate the initial response of the Elwha delta and nearshore environment to

Table 2

Instantaneous and cumulative volume change calculated from differences in DEMs; instantaneous change for May 2012 is calculated compared to August 2011; cumulative change is calculated compared to August 2011.

Survey	Instantaneous change			Cumulative change		
	Area (ha)	Change (m ³)	σ_{total} (m ³)	Area (ha)	Change (m ³)	σ_{total} (m ³)
Aug. 2011	–	–	–	–	–	–
May 2012	306.3	78,700	222,300	306.3	78,700	222,300
Aug. 2012	307.1	31,200	222,900	307.7	113,900	223,300
Mar. 2013	280.1	1,114,900	203,400	269.6	1,245,800	195,800
Sept. 2013	270.8	1,105,700	196,600	308.6	2,455,000	224,000

increased sediment delivery from the river. Model hydrodynamics were validated with in-situ field data from the tripods, and sediment dispersal and accumulation were validated against measured elevation change. Details of the model set-up, validation, and simulations are provided in the Supplemental section of this paper.

4. Results

4.1. Sediment volume and substrate change on beach and nearshore

4.1.1. Prior to dam removal

Repeat measurements of beach topography and nearshore bathymetry from 2009 through 2011 reveal the state of the delta in the two years prior to dam removal (Fig. 4). Delta morphology changed little during this time, though there were isolated areas of notable erosion and deposition (Fig. 4C). Changes within the river mouth include channel migration inside the estuary, as well as erosion of a river mouth bar and deposition farther offshore (Fig. 4D). Net volume change in the area of the river mouth was $\sim 47,000 \text{ m}^3$ of deposition between 2009 and 2011, or an average of $23,500 \text{ m}^3/\text{y}$. This volume of accumulated sediment compares to $34,000 \text{ m}^3$ of sediment deposited after the December 2007 flood event (Gelfenbaum et al., 2009; Draut et al., 2011).

East of the river mouth, the intertidal beach lost $\sim 45,000 \text{ m}^3$ of sediment between 2009 and 2011, resulting in $\sim 40 \text{ m}$ of landward migration of the shoreline (Fig. 4C and E). Erosion of the beaches on the east side of the delta has been ongoing for decades (Warrick et al., 2009a). By contrast, the beaches and nearshore west of the river mouth were stable between 2009 and 2011 (Fig. 4C), a pattern that is also consistent with long-term trends (Warrick et al., 2009a).

4.1.2. First year of dam removal

Measurable changes in delta morphology (Figs. 5–8) and grain size (Fig. 9) occurred following initiation of dam removal and continued throughout the first two years of monitoring. During the first year,

$113,900 \text{ m}^3$ of net sediment deposition was detected in the beach and seafloor (Table 2), representing roughly 5 times the annual background amount. This sediment accumulated in two distinct areas: (i) in front of the river mouth resulting in almost 100 m of progradation and steepening of the active delta front (Figs. 6A, 7C) and (ii) on the seafloor east of the tip of the subaerial delta (Fig. 6A). The majority of sediment accumulation in these two deposits (78%) occurred at subtidal elevations between -8 and -1 m (Table 3; Fig. 8). No detectable accumulation occurred on the seafloor between these two areas of deposition.

Despite the increase in sediment accumulation on the delta near the river mouth, beach erosion continued and was most pronounced on the upper foreshore east of the river, resulting in an alongshore-average shoreline retreat of 6.9 m and a maximum of 33 m during the 2011–2012 winter (Fig. 7E). Throughout the study area, erosion was concentrated around the MHW contour (Fig. 8) with a total of $41,400 \text{ m}^3$ of sediment erosion at intertidal and subaerial elevations.

Sediment grain size on the surface of the new deposit varied spatially across the deposit. In August 2012, the main deposit off the river mouth was composed of gravel and coarse sand, fining to medium and fine sand as the deposit thinned eastward (Fig. 9A and B). The secondary deposit located offshore of the east side of the subaerial delta was composed predominately of fine sand. Deeper portions of the subaqueous delta were composed predominately of gravel and coarse sand (Fig. 9A).

4.1.3. Second year of dam removal

During the second year, $2,221,000 \text{ m}^3$ of net sediment deposition was detected in the beach and seafloor (Table 2), with significant seasonal changes in location of the accumulation and in morphology. During autumn and winter of the second year of dam removal (August 2012 to March 2013), a time period that included the draining of Lake Mills and several river discharge events (Fig. 2), a total volume increase of $1,115,000 \text{ m}^3$ was measured with the majority of sediment accumulating offshore and just east of the river mouth (Fig. 6C). This deposit

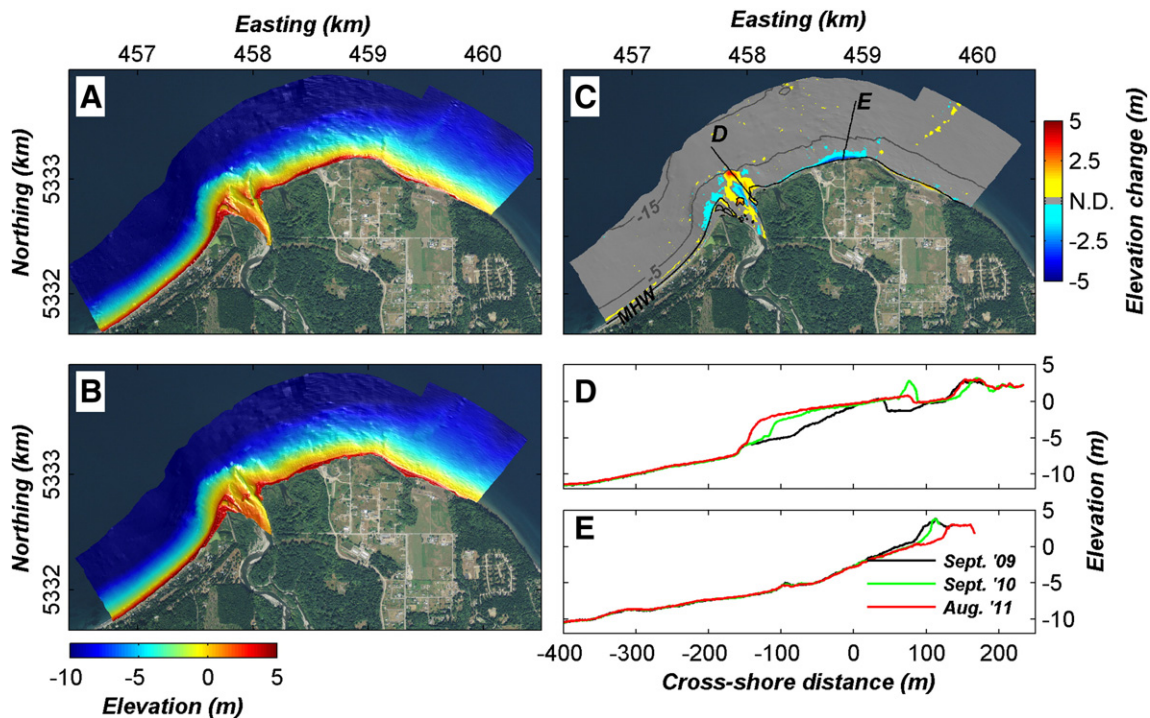


Fig. 4. Pre-dam removal morphology and elevation changes at the river mouth and adjacent beaches. (A) DEM from September 2009; (B) DEM from August 2011; (C) elevation change between September 2009 and August 2011. N.D. stands for not detectable and is $\pm 0.2 \text{ m}$; (D) and (E) cross-shore profiles along transects marked D and E in panel (C).

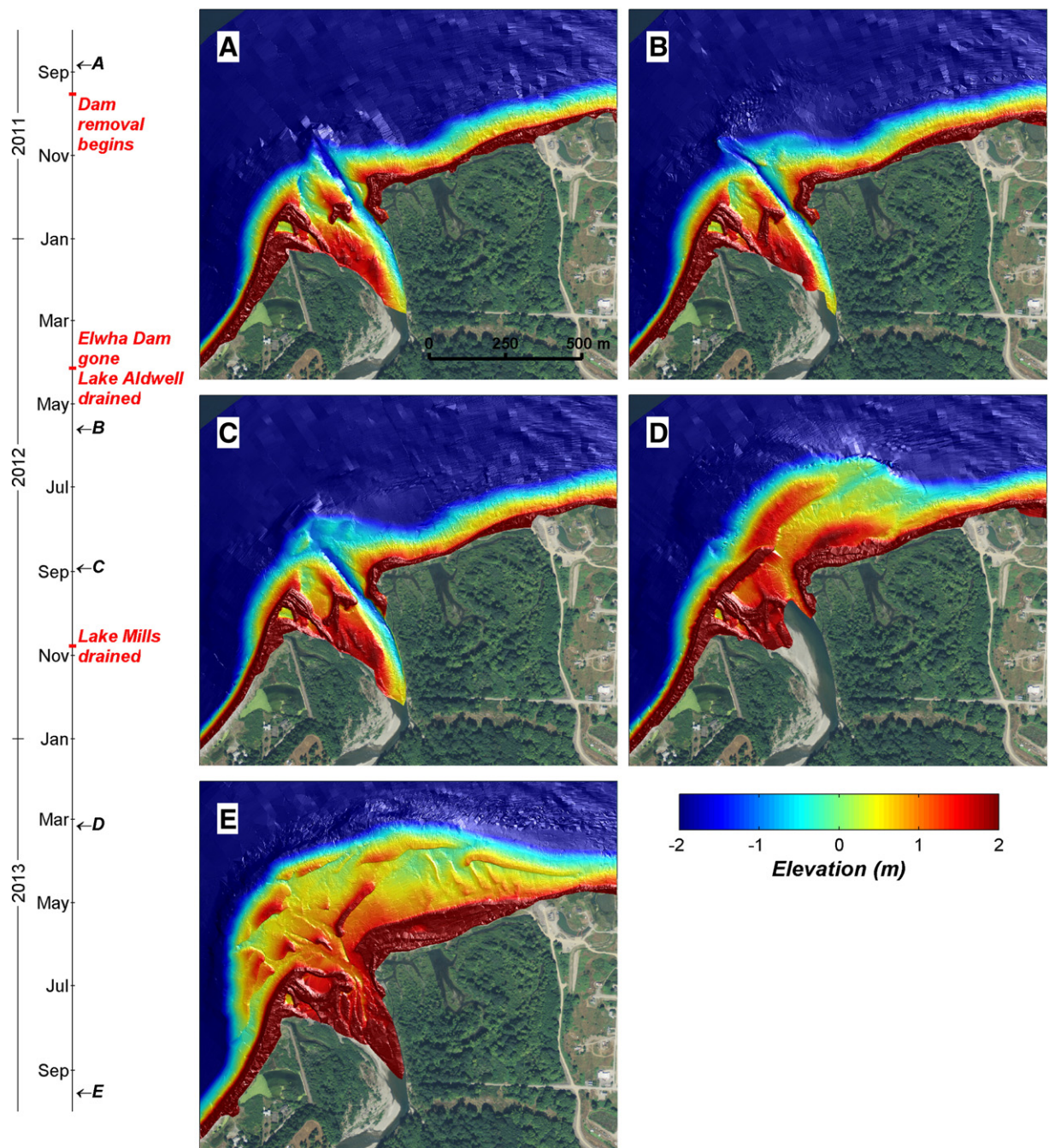


Fig. 5. Maps showing the geomorphic evolution of the active delta before and during the first two years of dam removal. (A) August 2011; (B) May 2012; (C) August 2012; (D) March 2013; (E) September 2013. DEM resolution is 1 m.

included an eastward-trending subaerial bar attached to the shoreline west of the river mouth and a large subaqueous bar that extended farther eastward, parallel to the shoreline (Fig. 5D). The shape of the outer active deposit was continuous and smooth suggesting that winter waves had caused the deposit to take on a more classic wave-dominated morphology. These features diverted the main river channel with its freshwater and suspended sediment load to the east (parallel to the coast), especially at lower tide levels. Sediment accumulation off the river mouth extended the active delta over 200 m offshore, pushing the toe of the new deposit to -10 m water depth (Fig. 7C). The front of this new inner delta grew vertically by as much as 7.5 m during this time period.

The main zone of accumulation extended primarily east of the river mouth and thinned to an undetectable thickness (<0.2 m) ~ 1 km away

from the river mouth (Fig. 6C). As during the first year of dam removal, sediment also accumulated in a second zone on the east side of the subaerial delta, and no significant accumulation was measured in between these two areas of deposition. Associated with this period of growth of the active delta, the shoreline immediately east of the river mouth prograded an average of 40 m, with a maximum progradation of 95 m (Fig. 7A and D). During this same time period, the beaches farther east of the river mouth on the tip of the subaerial delta continued to erode (Figs. 6C and 7E).

West of the river mouth and disconnected from the main depositor, an elongated area of deposition with an average thickness of 0.3 m was measured (maximum thickness of 1.2 m) in water depths of -1 to -3 m (Figs. 6C and 7B).

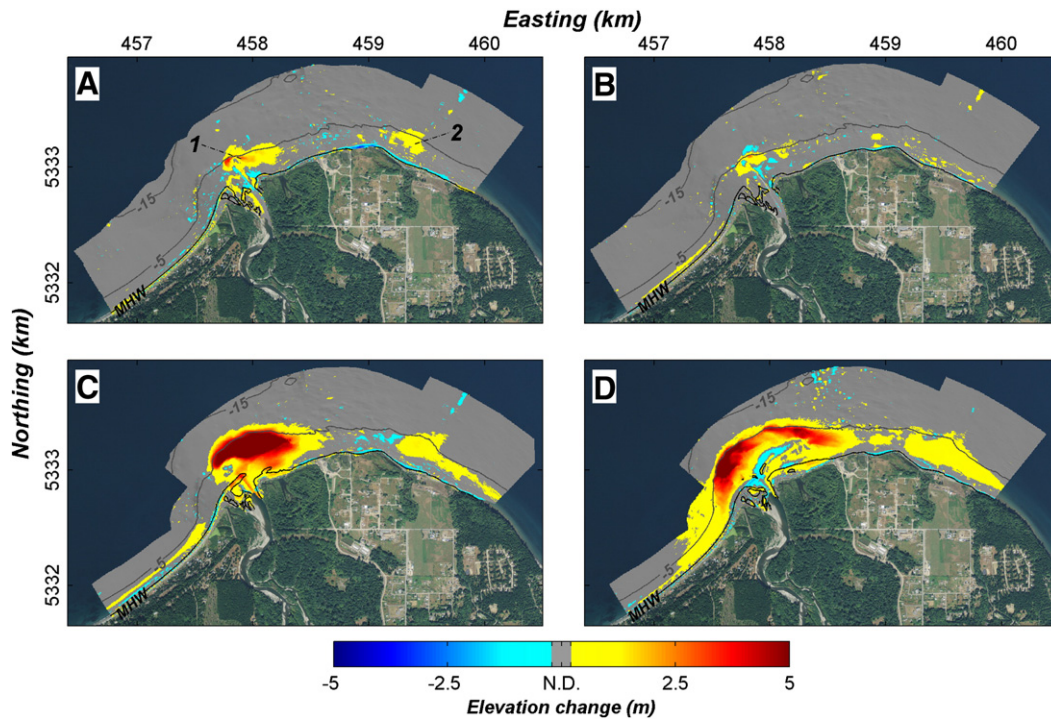


Fig. 6. Maps showing elevation change between surveys. (A) August 2011 to May 2012; (B) May 2012 to August 2012; (C) August 2012 to March 2013; (D) March 2013 to September 2013. Reds represent deposition, blues are erosion, and gray represents regions with no detectable change (N.D.) between surveys. Thin black line represents the mean high water (MHW) shoreline, gray lines are -5 and -15 m bathymetric contours. The primary (1) and secondary (2) areas of deposition are denoted in (A).

During the latter half of the second year of dam removal, from March 2013 through September 2013, an additional $1,106,000 \text{ m}^3$ of sediment accumulated offshore of the river (Fig. 6D). The thickest part of the new deposit accumulated just west of the river mouth, extending the active delta 140 m offshore into water depths of 12 m (Fig. 7C). Farther west of the river mouth, significant new deposition was measured for the first time in water depths to -15 m (Figs. 6D and 7B). This new deposit was thin ($<2 \text{ m}$ thick) and connected to the foreshore. The zone of secondary deposition offshore of the east side of the subaerial delta continued to grow with the addition of $115,000 \text{ m}^3$ of sediment.

Close to the river mouth, a river channel cut through the bar that had been attached to the beach from the west side. By September 2013, no single channel exited through the delta (Fig. 5E) but instead there were several bifurcated channels separated by bars; also, a series of transverse bars formed parallel to shore on the east side of the active delta. This irregular, bisected outer deposit shape suggests a transition to a more classical river-dominated morphology. Unfortunately, the twice per year mapping was not able to capture all of the transitions in delta morphology that occurred as wave and river discharge conditions changed more frequently.

By September 2013 the main deposit just off the river mouth became more coarse, composed predominately of gravel and coarse sand (Fig. 9C and D). As the deposit thinned eastward, it continued to fine and was composed of medium and fine sand. As the secondary deposit off the east side of the delta grew larger and spread eastward, it also grew finer and was composed of fine sand and mud. In shallow near-shore regions west of the river mouth, a thin deposit formed composed of fine sand and mud.

4.1.4. Net changes during first two years of dam removal

The total beach and nearshore volume change in the first two years of dam removal from August 2011 through September 2013 was $2,455,000 \text{ m}^3$ (Fig. 7; Table 2). The majority of that accumulation was located immediately offshore of the river mouth and extended the active

delta over 200 m northward and steepened the front of the new deposit. The portion of the river mouth and delta where the majority of sediment accumulated changed location from the first year to the second year. During the first year of dam removal, over 78% of the sediment accumulated in shallow subtidal depths between -1 and -8 m MLLW (Table 3) and the maximum accumulation occurred around -2.4 m (Fig. 8B). During the second year, a similar total percentage of sediment accumulated at subtidal elevations (81%), but the elevation of maximum accumulation was at a higher elevation than during the first year, at approximately MLLW (Fig. 8B).

Areas of new deposits thinner than 20 cm , the between-survey measurement uncertainty (Table 1), could have gone undetected. Specifically, west of the river mouth between -10 and -20 m depth, no accumulation was detected in the elevation change maps, yet acoustic backscatter intensity maps and sediment texture changes suggest deposition of new sediment. This region of low acoustic backscatter, as seen in the March 2013 swath survey (Fig. 10b), corresponds to a region where seabed sampling revealed changes in sediment texture. Prior to and in the first year of dam removal, sediments in this area were composed primarily of gravel, coarse sand, and medium sand (Fig. 9A and B). By the end of the second year of dam removal, this region began fining to medium sand, fine sand, and mud (Fig. 9C and D) (Eidam et al., 2014) (see Supplemental documents for more details). Beyond about 25 m water depth, grab samples indicate that little to no sediment deposited on deeper portions of the relict, subaqueous delta (which extends to a slope break at $\sim 60\text{-m}$ water depth; Fig. 1).

4.2. Detailed temporal shoreline and beach substrate changes

Biweekly sampling of beach grain size and topography along three cross-shore-oriented transects helps to resolve the timing and arrival of a new sediment onto the beaches, especially for periods of time in between biannual bathymetric and topographic surveys (Fig. 11). West of

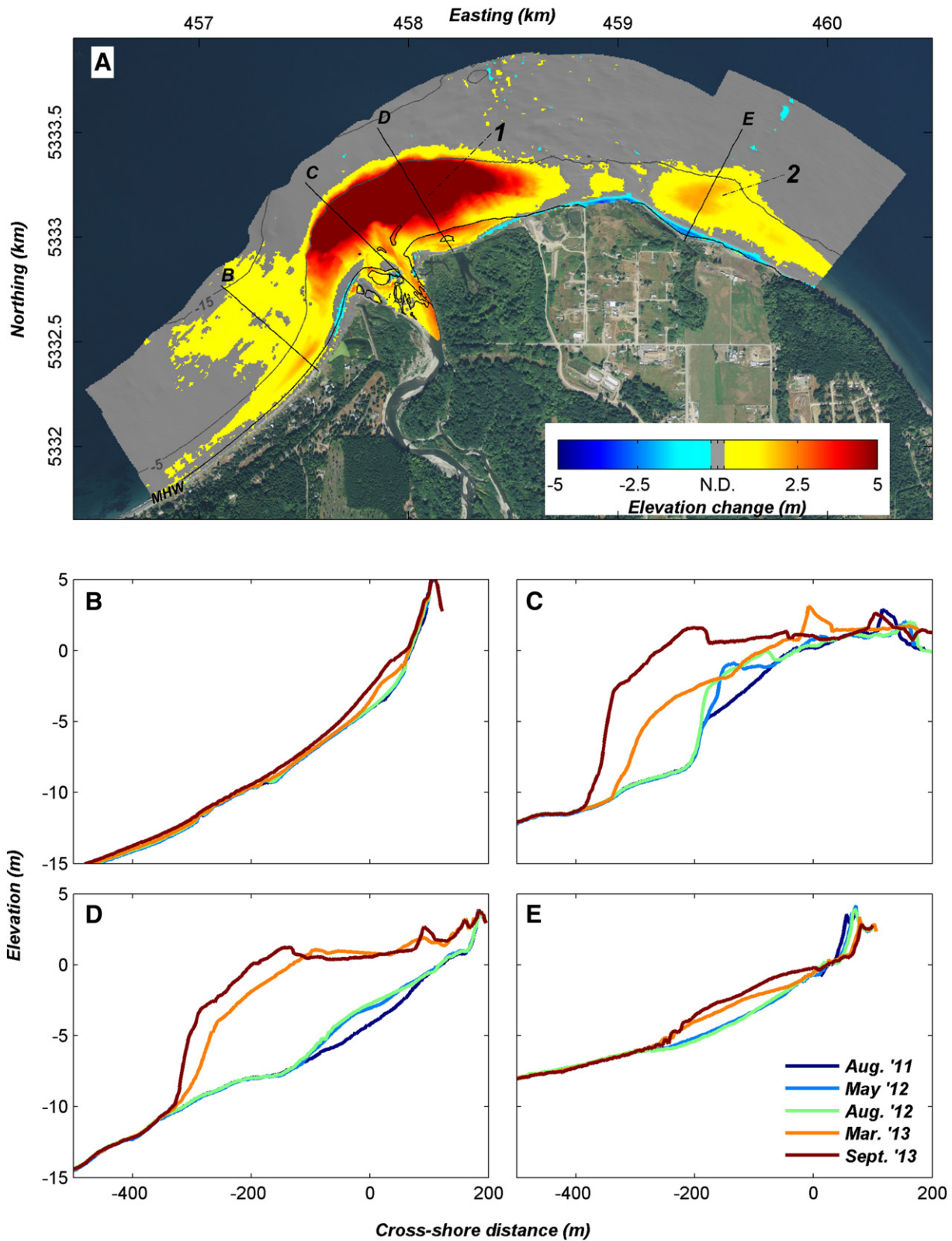


Fig. 7. (A) Cumulative beach and seafloor change between August 2011 and September 2013. (B–E) Profiles of bathymetry and topography along selected transects shown in (A). See Fig. 6 caption for detailed description of elevation change map.

the river mouth, the position of the MHW contour was mostly stable through the first two years of dam removal, migrating seaward only about 6 m from September 2011 until September 2013 (Fig. 11A). The beach progradation increased while the median foreshore grain size

decreased from ~30 to ~5 mm in early summer of 2013, coincident with the removal of Aldwell Dam.

At a transect 350 m east of the river mouth, there was a temporary reduction in beach grain size during the spring of 2012 associated

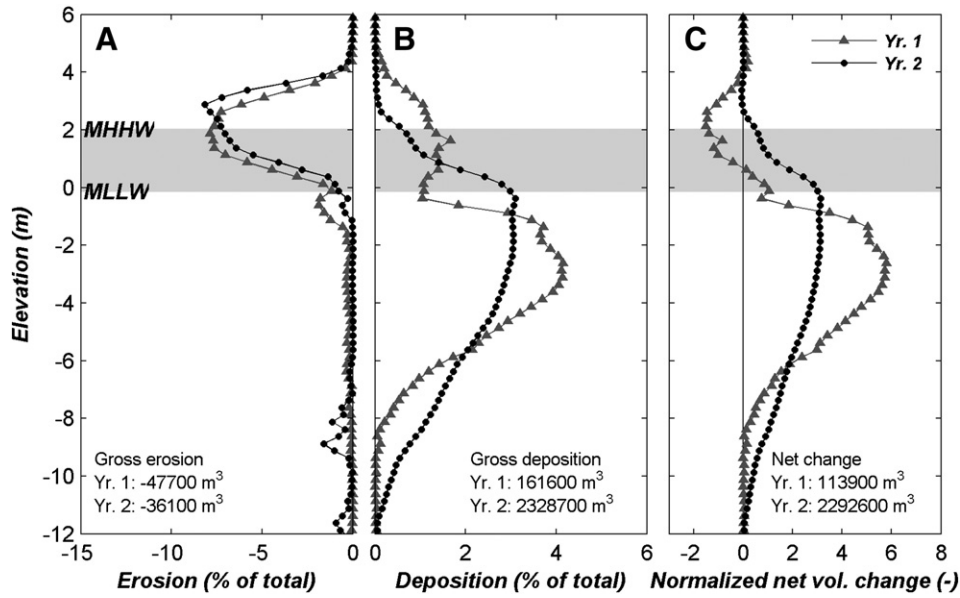


Fig. 8. Elevation at which sediment was (A) eroded, (B) deposited, and (C) normalized net change. Volume changes were calculated between August 2011 and August 2012 (year 1, gray triangle) and between August 2012 and September 2013 (year 2, black circle) and normalized by the total gross erosion, deposition, and net volume change.

with the removal of Elwha Dam, despite a lack of shoreline change (Fig. 11B). Starting in early 2013 there was a rapid morphologic response of the beach, as evidenced by the abrupt decrease in median grain size and progradation of the MHW line. This response roughly coincided with the draining of Lake Mills (Fig. 2) and is associated with

delta growth immediately seaward of the river mouth (Fig. 6C). Farther eastward, the foreshore at the transect 960 m east of the river mouth had little measurable morphologic response to dam removal, with steady beach erosion, and large mean beach grain size persisting throughout the two-year study period (Fig. 11C).

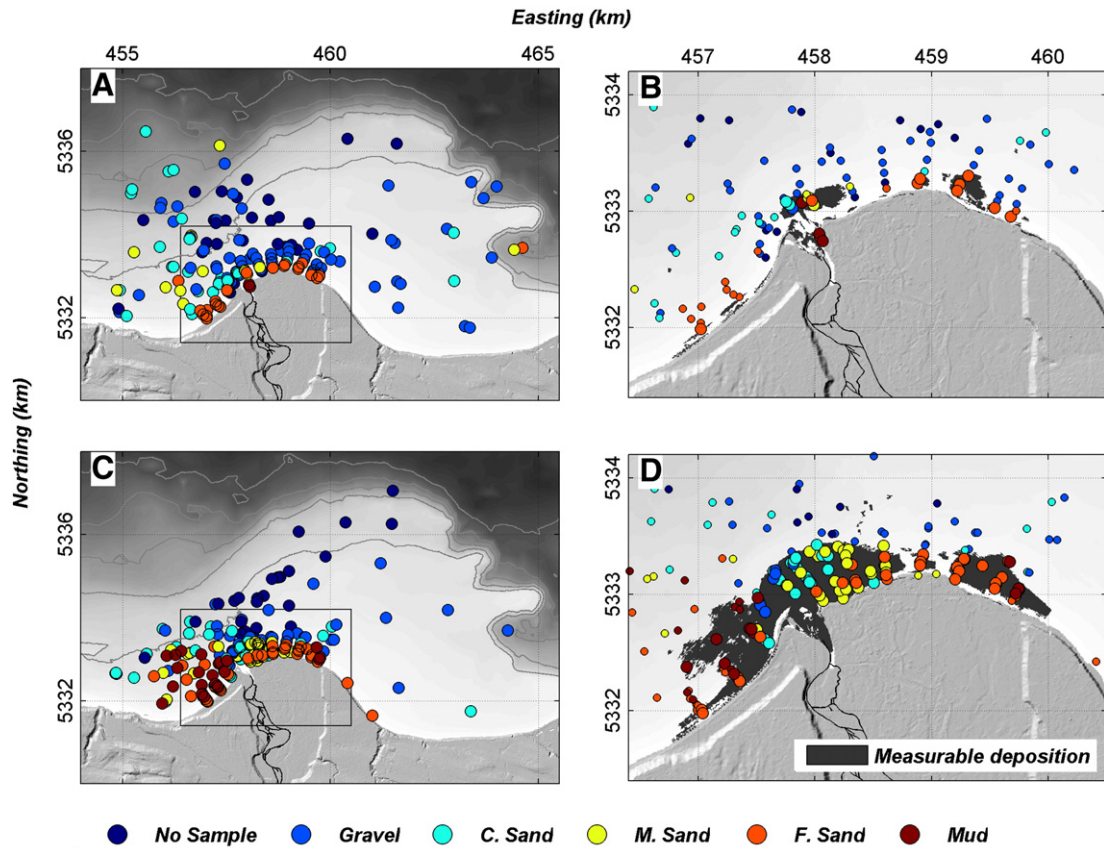


Fig. 9. Maps of seabed mean grain size across the submarine delta during (A) and (B) the first year of dam removal, and (C) and (D) the second year of dam removal. The dark blue circle labeled no sample is interpreted to represent hard ground or a substrate so coarse that a sample could not be collected. The black box in (A) and (C) is the area expanded in (B) and (D). Area marked measurable deposition derives from the difference map shown in Fig. 7A.

Table 3
Volume of erosion, deposition, and net volume change occurring at different depths throughout the study area; volume eroded or deposited as a percent of total reported within parentheses.

Depth	Erosion (m ³)		Deposition (m ³)		Net change (m ³)	
	Year 1	Year 2	Year 1	Year 2	Year 1	Year 2
Subaerial	–19,300 (48)	–18,200 (57)	11,700 (9)	28,300 (2)	–7500	10,200
Intertidal	–22,100 (40)	–12,900 (29)	19,300 (12)	347,500 (17)	–2800	334,600
Subtidal	–6300 (11)	–5000 (14)	130,600 (78)	1,952,900 (81)	124,300	1,947,900

5. Discussion

5.1. Sediment budget and temporal evolution

One of the goals of this research is to calculate a sediment budget to help assess the effects of dam removal on the adjacent coastal system. A sediment budget will characterize the quantity and timing of coastal deposition relative to river sediment supply. Because river sediment supply and coastal deposition are measured in units of mass and volume, respectively, an estimate of the dry bulk density of the deposit is required to convert sediment volume to sediment mass. The bulk density of the deposit is not a constant in time or space, however, as the conversion depends on the water content or porosity of the deposit, which in turn depends on the sediment grain size distribution and the level of compaction in the bed. We did not quantify the amount of compaction in the deposit, but used the spatially explicit map of measured surface grain size (Fig. 9) to estimate the porosity and thus the dry bulk density. Following the method of Allersma (1988) and using Eq. 3.2.7 in van Rijn (2005) to calculate bulk density as a function of percent sand, and with a compaction coefficient of 1.0, we calculate the mean dry bulk density (and range) to be 1470 (1430–1500) kg/m³ for the August 2012 survey;

1410 (1120–1490) kg/m³ for the March 2013 survey; and 1360 (690–1500) kg/m³ for the September 2013 survey.

Comparison of the mass of fine (clay- and silt-sized) and coarse (sand- and gravel-sized) sediment deposited in the coastal zone to the mass of sediment transported by the river (Fig. 12) shows how much sediment is found (or lost) in the coastal zone. By the end of the first year after dam removal began, about 570,000 tonnes of fine sediment was transported down the river, but only about 8000 tonnes was found within the DEM survey area. By the end of the second year after dam removal began, about 3,400,000 cumulative tonnes of fine sediment was transported down the river, but only ~200,000 tonnes, or <6% of the mass delivered, can be identified in the shallow regions of the delta. A small fraction of the remaining 94% could be on the seafloor in thin deposits undetected by the repeat bathymetric surveys, as is suggested by the March 2013 acoustic backscatter map (Fig. 10B). The area of low backscatter intensity west of the river mouth where fine-grained sediments were found (Fig. 9), and which was less than the detection limit of bathymetric change, is only about 56 ha. Assuming a mud density of 690 kg/m³, this sediment deposit is estimated to represent about 73,000 tonnes, or 2% of the total fine-grained sediment transported down the river. The majority of fine sediment was more likely dispersed far from the Elwha River mouth, outside of the region mapped. Using a long-term morphological simulation, Gelfenbaum et al. (2009) predicted that some fine-grained sediment would ultimately be deposited far from the Elwha River mouth off the east side of the larger submarine delta or inside the tip of Ediz Hook at the entrance to Port Angeles harbor. Observations to date, however, are unable to verify those predictions.

Unlike the fine sediment, most of the sand- and gravel-sized sediments delivered by the river can be accounted for within the area mapped during the first two years of dam removal (Fig. 12). During the first year about 500,000 tonnes of sand and gravel was transported down the river, and the DEM difference maps identified 230,000 tonnes. By the end of the second year, a total of 4,800,000 tonnes of sand and gravel was transported down the river, and 3,300,000 tonnes was identified in the survey area, or about 70%.

Several sources of uncertainty in the sediment budget limit the comparison between the river source and the coastal accumulation volumes after dam removal. Uncertainty exists in the volume change estimates arising from the systematic errors in elevation mapping (Table 1), but this error is small compared to that associated with other sources. One of the larger sources of error in the sediment budget is the estimate of the dry bulk density, which was derived from the grain size distributions of surface grab samples. Thus, this estimate includes uncertainty in the percentage of fine versus coarse sediment, porosity and compaction of the deposit, and the within-deposit variations in these factors. Accounting for the uncertainties in the bulk density, compaction, and systematic uncertainty in elevation measurements, we estimated the possible range of coarse sediment accumulating in the coastal zone after two years to be 2,400,000–3,900,000 tonnes (Fig. 12).

Estimates of the river sediment supply, likewise, have several sources of uncertainty. One source of uncertainty in the sediment supply to the coast derives from the deposition of sediment in the lower river below the gaging station. East et al. (2015) estimated 289,000 tonnes of sediment accumulated over the two years along the lower river downstream of the Elwha Dam. This estimate, which is small

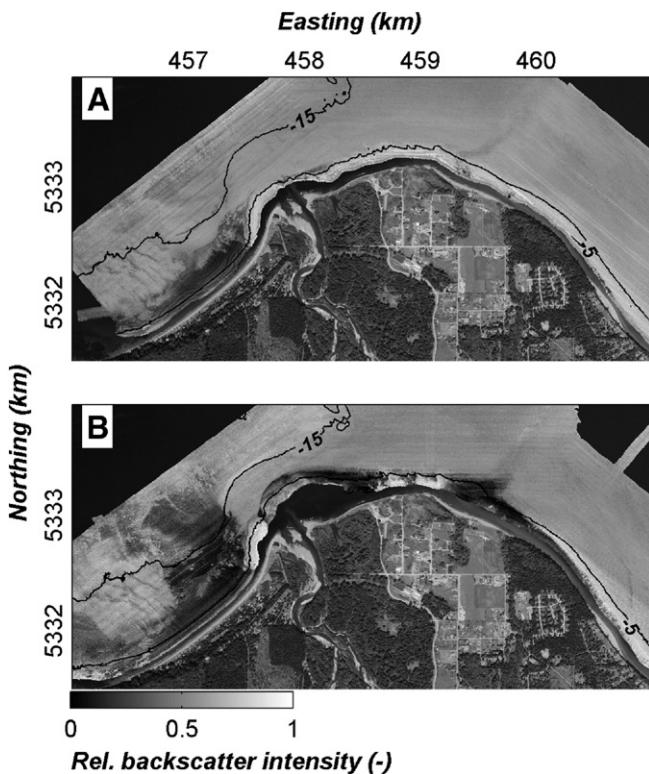


Fig. 10. Acoustic backscatter from SwathPlus sidescan sonar data collected in (A) February 2010, before dam removal and (B) April 2013, after dam removal. Dark areas represent lower backscatter intensity, which is associated with finer sediments. Bright areas represent higher backscatter intensity, which is associated with hard bottom or coarser sediments.

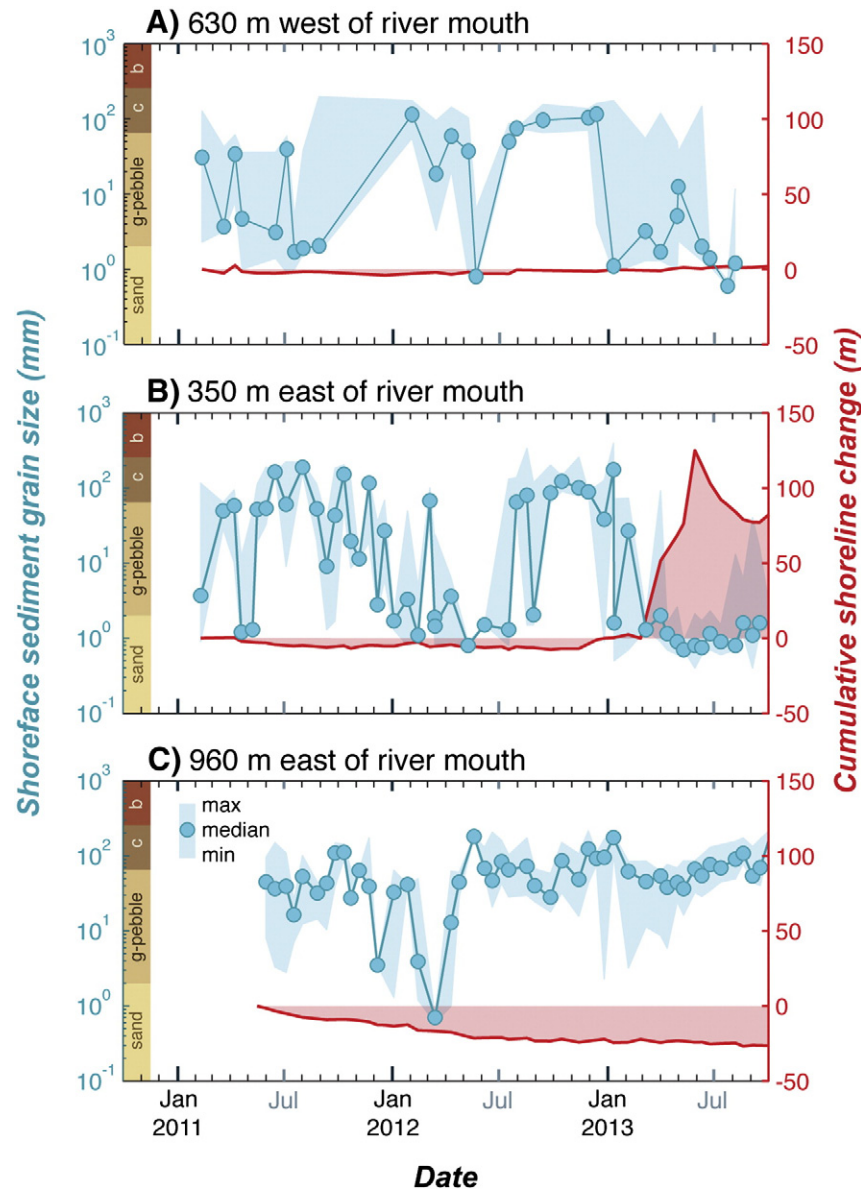


Fig. 11. Changes in shoreline position and sediment grain size during the first two years of dam removal at transects located (A) 630 m west of the river mouth; (B) 350 m east of the river mouth; and (C) 960 m east of the river mouth. Refer to Fig. 3 for map showing transect locations. Median and range of sediment grain sizes are shown for samples collected biweekly at 0.25-m elevation intervals on the intertidal shoreface between 1.0 and 2.5 m NAVD88. Sediment grain size classes from Wentworth scale with c = cobble and b = boulder.

compared to the uncertainties in measurement and in the impact of the bulk density, does not account for all of the floodplain deposition and is based on surveys that do not distinguish between mud and coarser sediment (East et al., 2015).

Uncertainty derived from measurements of bedload and suspended load in the river, which are discussed in detail in Magirl et al. (2015) are even larger. They report difficulties measuring bedload in rivers like the Elwha, especially for the sand-sized sediment transported near the bed. For the two-year period after dam removal began, they estimated 1,950,000 tonnes of bedload passed the gauging station, with an uncertainty of nearly 88%. Their estimates of uncertainties in suspended load are much smaller, at around 50% of the estimated 6,300,000 tonnes.

In addition to quantifying the volume (or mass) of sediment redistributed from the watershed to the coast during dam removal, we can also comment on the timing of the response of the coast to the increase in sediment supply, and where within the coastal system that response occurred. Because the dam removal process was staged over months and was not instantaneous (like the Condit Dam removal, for

example; Wilcox et al., 2014), the amount of sediment released from the reservoirs transported down the river did not dramatically increase immediately after dam removal began (Fig. 2). Likewise, the amount of sediment that accumulated in the delta and along the adjacent coast was small during the first year and was much larger the second year (Figs. 11 and 12).

The increase in magnitude of sediment deposition between the first and second year was accompanied by a change in the location of the delta where the majority of sediment accumulated (Table 3; Fig. 8). This switch in the location of deposition on the delta over time is probably a result of the timing of delivery of sediment to the river-mouth region and how the morphology of the river and the estuary affect the strength of the flow at the mouth of the river. During the first year, the river flowed through a single deep channel through the estuary, discharging the sediment load farther offshore of the river mouth on the flanks of the active delta (Fig. 5A–C). As sediment load in the river increased in the second year, sediment deposited in the estuary and the river became shallower and the flow dispersed through multiple

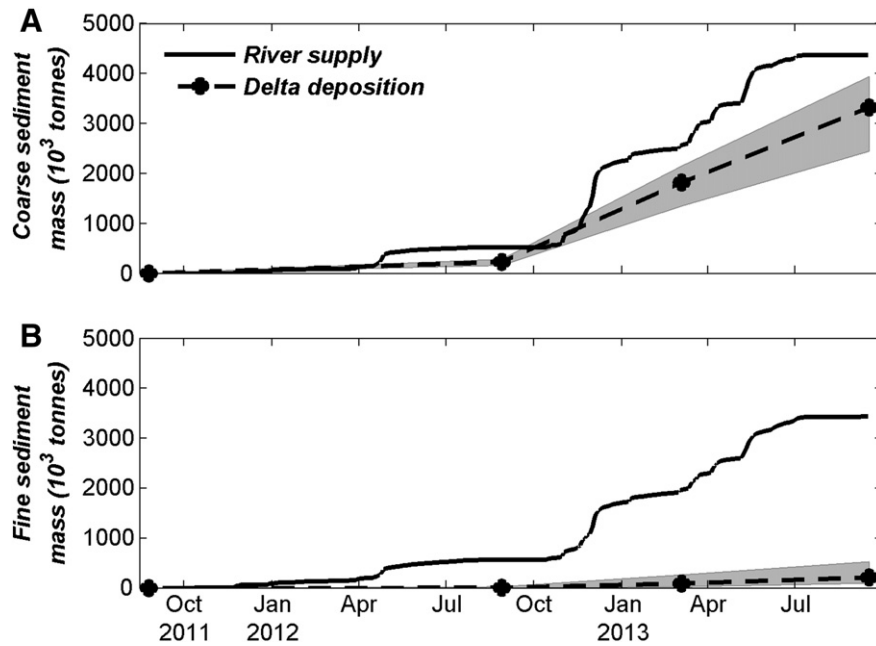


Fig. 12. Time series of mass of cumulative river sediment supply compared to mass of sediment accumulated on the delta for (A) coarse (sand–gravel) components and (B) fine (silt–clay) components. Gray-shaded area shows possible range in mass of sediment deposited resulting from uncertainty in bulk density and compaction and uncertainty in elevation measurements from Table 1.

channels. With lower flow speeds at the delta, the sediment deposited closer to the river mouth, building bars and expanding the intertidal delta (Fig. 5D–E). During most of this second year, the river never reached flood level flows and was not able to flush the accumulated sediment out of the estuary (East et al., 2015).

The detailed sediment budget results described here for the delta and coast are summarized in a systemwide sediment budget for the entire Elwha and reported in Warrick et al. (2015).

5.2. Sediment dispersal

5.2.1. Explaining complex patterns of deposition

One of the consequences of the removal of the Elwha River dams was the rapid increase in sediment loads in and through the fluvial system and an increased sediment supply to the coast. At the coast, tidal currents, waves, and river discharge influenced sediment dispersal pathways, resulting in complex patterns of deposition and grain size

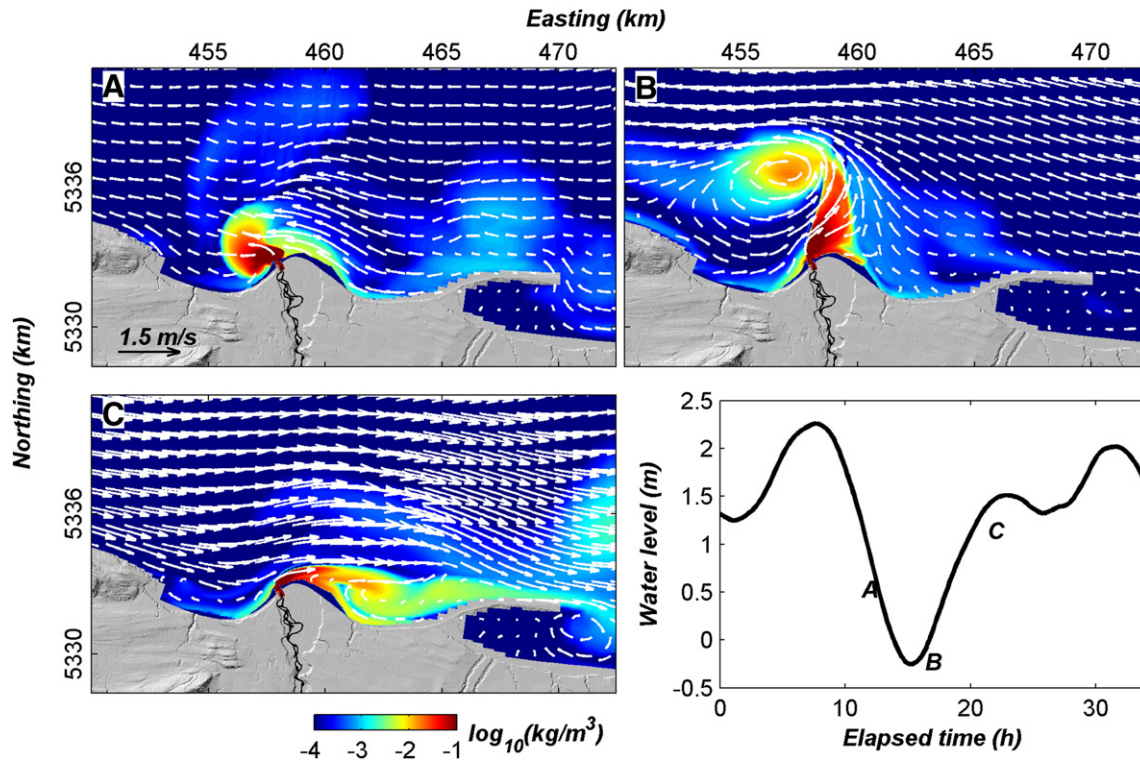


Fig. 13. Modeled sediment dispersal at various phases of the tide. Colors represent suspended sediment concentration and arrows show surface current speed and direction.

distributions. Here, we examine tripod ADCP and camera data, and simulations from the Delft3D hydrodynamics and sediment transport model to explain the processes responsible for the observed patterns of deposition and size-sorting of sediment.

A dominant control on sediment deposition is the irregular shape of the Elwha delta itself, which influences tidal current dispersal of the Elwha River plume (Warrick and Stevens, 2011) and enhances resuspension and advection of coarser sediment from the bed. As predicted by Signell and Geyer (1991) for tidal flow around headlands in general and by Warrick and Stevens (2011) for the Elwha River delta, the delta headland induces flow separation of currents. Flow around the headland produces large-scale transient eddies (Fig. 13) and strong (up to 0.4 m/s) residual currents (Fig. 14), both of which have been identified in tripod data and in model simulations validated against field measurements (Table 4). The tidal residual currents form two large coherent residual eddies: a counterclockwise eddy on the west side and clockwise eddy on the east side (Fig. 14). These eddies are not located symmetrically about the subaerial delta but are shifted eastward a few kilometers and are located more symmetrically about the larger and deeper subaqueous delta. Strong tidal currents direct the Elwha plume and entrained fine sediment toward Ediz Hook to the east and throughout much of Freshwater Bay to the west (Fig. 13). Tidal dispersal of the plume is responsible for transporting fine-grained sediments in suspension many kilometers across the region, similar to other tidally dominated systems—for example, the Mobile Bay plume in the northern Gulf of Mexico (Stumpf et al., 1993).

Table 4

Comparison between modeled and measured water level, depth-averaged velocity, significant wave height, and peak wave period at two sites within the Elwha model domain; RMSE is root mean square error, and d is the index of agreement (Willmott, 1982); model and data compared for the time period 1 April–20 May 2012.

Site	Parameter (units)	Mean (SD)		RMSE	d
		Model	Data		
Site E	Water level (m) ^a	0 (0.66)	0 (0.67)	0.13	0.99
	Depth-averaged velocity (m/s)	0.56 (0.35)	0.51 (0.38)	0.18	0.93
	Significant wave height (m)	0.43 (0.25)	0.45 (0.23)	0.22	0.78
	Peak wave period (s)	6.3 (2.5)	8.8 (3.2)	4.2	0.6
Site W	Water level (m) ^a	0 (0.66)	0 (0.66)	0.13	0.99
	Depth-averaged velocity (m/s)	0.15 (0.08)	0.14 (0.08)	0.08	0.72
	Significant wave height (m)	0.40 (0.24)	0.42 (0.23)	0.21	0.78
	Peak wave period (s)	6.7 (2.9)	9.4 (2.7)	3.9	0.6

^a Mean values were removed from model and data.

Although sediment is transported broadly over the submarine delta and beyond, observed sediment accumulation on the seafloor following dam removal was limited to shallow regions (mostly <12 m water depth; Fig. 7) and consisted primarily of sand and gravel, with mud accumulating in smaller proportions (Fig. 9). High boundary shear stresses from tidal currents along with strong residual flow limit sediment deposition over much of the submarine delta (Fig. 15). A time series of photographs of the seafloor at the East tripod in about 10-m water depth shows the passage of highly turbid waters, temporary deposition of

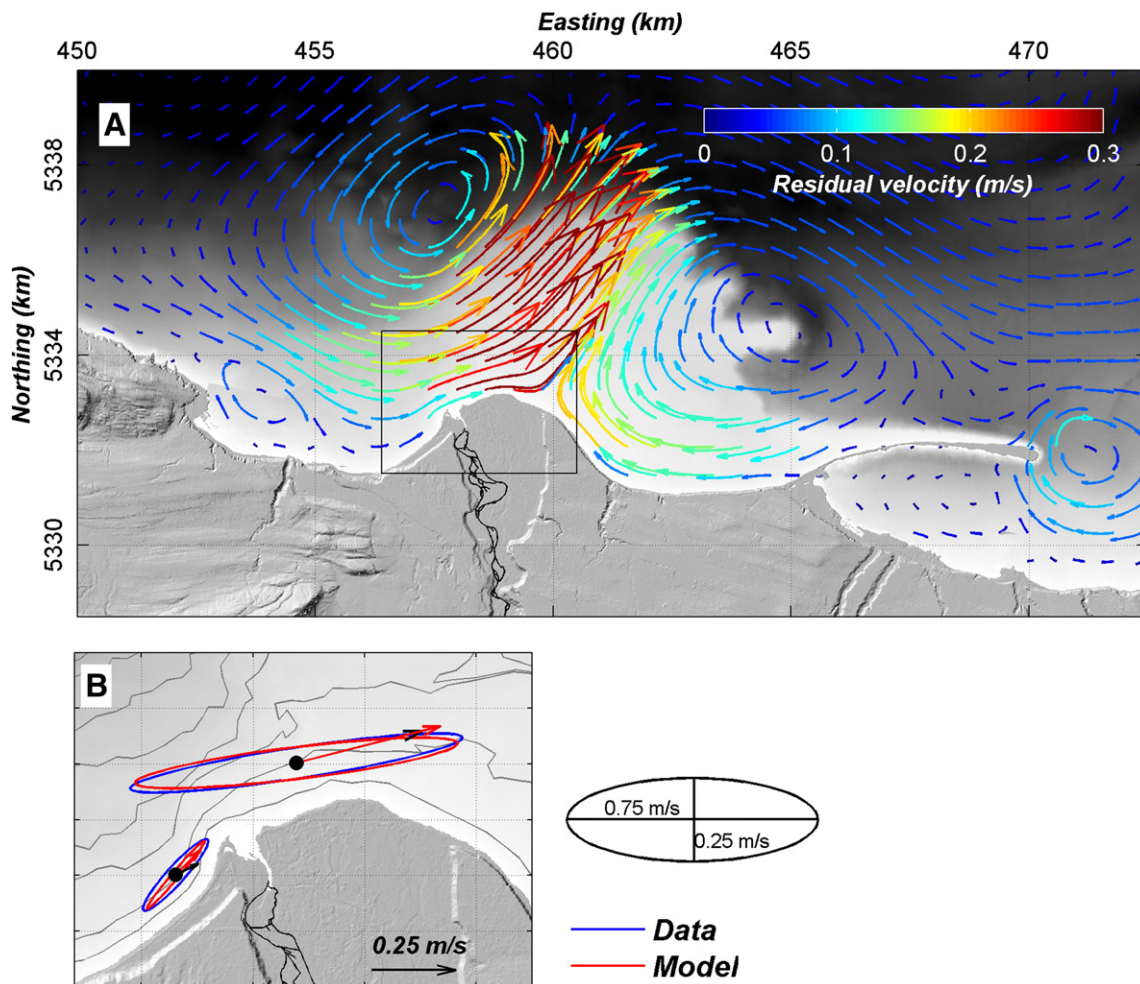


Fig. 14. (A) Modeled residual currents. The colors represent the magnitude of the residual current. (B) Comparison of modeled and measured depth-averaged current ellipses at the two tripod sites, E and W. Arrows represent residual mean currents. Red are model results, and blue are measured.

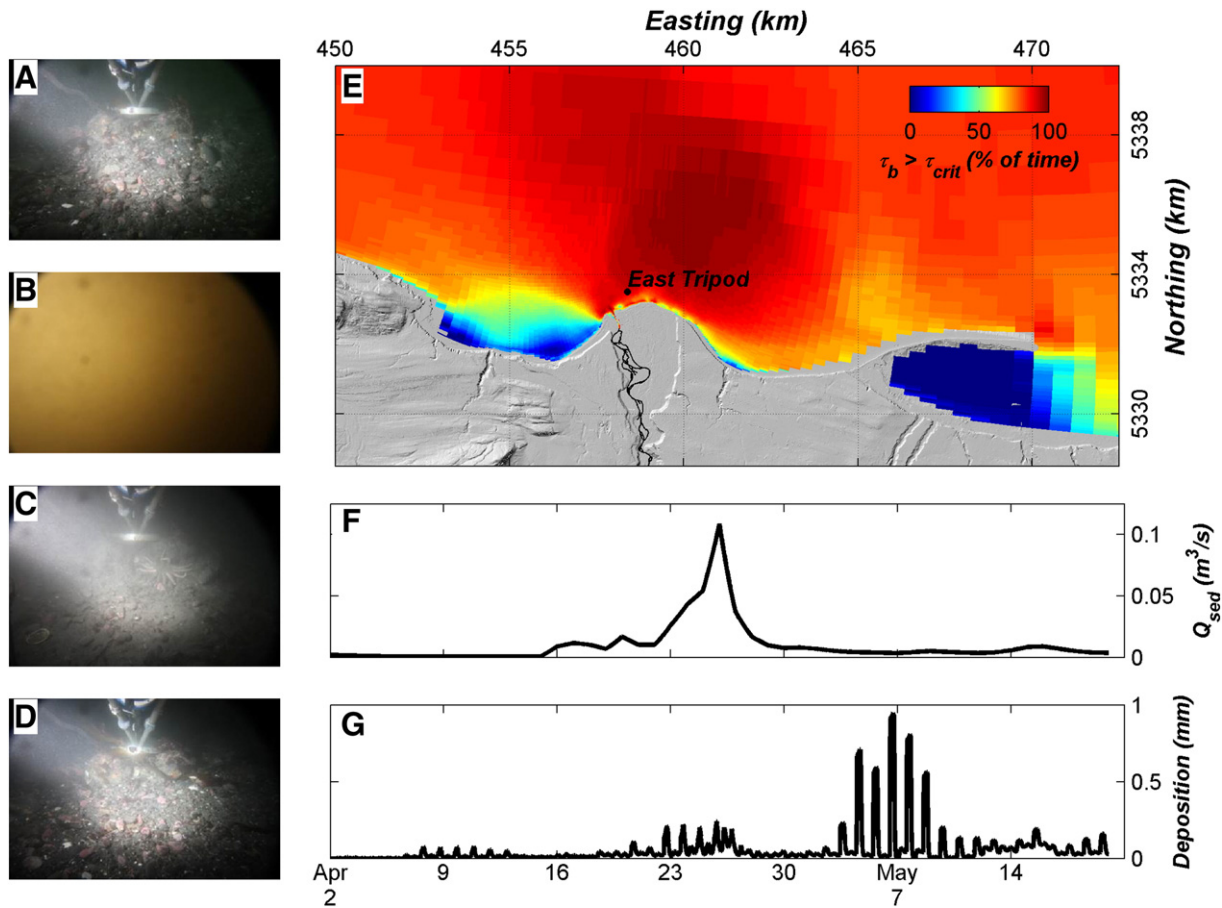


Fig. 15. (A–D) Time series of photos from camera on instrumented East tripod location. (E) Map of percent of time during the model simulation that boundary shear stress exceeds critical shear stress for 200- μ sand. Time series from April through May 2012 of (F) Elwha River sediment discharge and (G) modeled cumulative sediment deposition at the location of the East tripod.

fine sediment on the bed, then resuspension of the fine sediment, leaving the pre-existing coarse, armored bed (Fig. 15A–D). Resuspension and transport of the newly deposited sediment from the seafloor are common on the Elwha delta. A model simulation with waves and currents for the time period 1 April–20 May 2012 shows that boundary shear stress (τ_b) exceeds the critical shear stress for 200- μ sand ($\tau_c = 0.18$ Pa) more than 50% of the time across most of the delta and more than 80% of the time across the central delta (Fig. 15E). Over the central portion of the delta, at the East tripod site for example, where the boundary stress is almost always greater than the critical stress for sand and residual currents are strong, a time series of modeled cumulative deposition and erosion shows that sediment is deposited only temporarily and then rapidly erodes, leaving no net deposition (Fig. 15G). Even in areas where deposition was observed, preferential resuspension of available fine sediment (e.g., Law et al., 2007) resulted in mostly coarse sediment deposits. Only in Freshwater Bay west of the river mouth, where bottom stresses are relatively low and residual currents are weak, are there sufficient periods of reduced bottom stress to allow fine sediment to settle and accumulate. This region corresponds to the region of measured fine sediment accumulation west of the river mouth (Fig. 9).

The complex sediment transport processes can be simulated with the numerical model to better understand the patterns of deposition observed in the data (Fig. 16). In this comparison of observed and modeled sediment deposition, the model was run from 3 April to 20 May 2012, the initial part of dam removal when sediment loads were increasing, but still not at their maximum (Fig. 2). In the observations and in the model, coarse sediment is deposited in two areas. The primary area of deposition occurs directly off the river mouth where the supply, at least temporarily, overwhelms the capacity of coastal processes to

transport it. Strong tidal currents regularly resuspend sediment from the primary deposit off the river mouth, and residual currents result in eastward transport along the inner delta. The model suggests that sediment bypasses the central region of the delta and that the secondary area of deposition occurs on the eastern side of the delta where the tide-induced residual currents converge and are weak (Fig. 14). In the model, very little deposition of fine sediment was observed as high stresses and strong net transports efficiently carried fine sediment out of the model domain.

5.2.2. Effects of waves and river floods on sediment dispersal

Though tidal processes are the primary control over sediment dispersal on the delta, waves (wave resuspension) and river floods are important transport processes that augment or modify sediment dispersal. We can use the validated hydrodynamics and sediment transport model to demonstrate the effects of wave resuspension and river floods on sediment dispersal. To demonstrate the importance of waves, two sediment transport simulations were run, both identical, except one included wave processes and one did not (Fig. 17A and C). For the nearly two-month simulation with waves, significant wave heights on the delta at the 10-m tripod location exceeded 1 m six times with a maximum height up to 1.4 m (Fig. 17B). Wave periods varied between 3 and 14 s, and waves were always from the northwest. Without waves to help resuspend the 200- μ sand on the inner delta in the no-wave simulation, the mean sediment transport rates across the inner delta were about a quarter to a half the transport rates when waves were included. Even though the pattern of dispersal was the same because of the dominance of the tidal processes, waves enhance the boundary shear stress on the inner Elwha delta, increasing sediment resuspension and

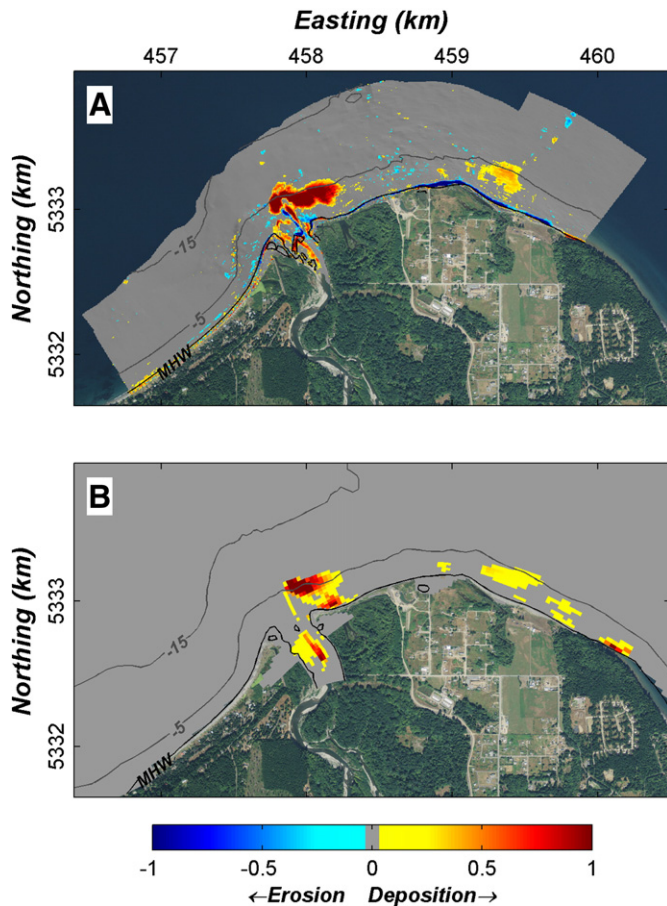


Fig. 16. Comparison of (A) observed and (B) modeled initial sediment accumulation. Measured accumulation is between September 2011 and May 2012; modeled accumulation from simulation run between April 2012 and May 2012. Reds are deposition and blues are erosion.

promoting advection by tidal currents. Although not modeled in this simulation, waves are also responsible for driving alongshore transport of sediment on the foreshore. As shown by Miller et al. (2011) and Miller and Warrick (2012), wave height is highly correlated with sediment transport, predominately eastward, along the beaches of the Elwha River delta.

To demonstrate the importance of river flood events on sediment transport pathways, we ran two identical simulations, except one with a constant river discharge and one with a time varying discharge (Fig. 17A, B, and D). In both simulations the same total sediment load was delivered to the coast, but in the constant discharge case there were no flood events to push the sand farther offshore. Instead, all of the sand was delivered to the inner portion of the delta, closer to the river mouth. There are examples (e.g., Wright, 1977; Wheatcroft et al., 1997) that show that large flood events can deliver fine sediment farther offshore, however the effect on coarser sediment delivery to the coast and resulting delta morphology is less well understood. For the Elwha, the effect of a flood event on sediment transport pathways across the inner delta may be significant (Fig. 17A and D). In the paired simulations, the higher river discharge during flood events delivers more sand-sized sediment to a deeper portion of the inner delta (Fig. 17A) than if there were no flood (Fig. 17D). With more sand on the outer part of the inner delta, there is more sediment transported eastward along deeper contours than if the sand were deposited on the inner part of the delta where tidal currents decrease. This small

difference in where sand is delivered by a flood makes a large difference in the sand transport pathways along the inner delta.

5.3. Substrate and habitat changes

Prior to dam removal, hydrodynamics over the delta and sediment supply limitations induced by river damming influenced the substrate of the Elwha delta seafloor. Strong tidal currents and long-period waves combined to produce high bottom boundary shear stresses (Fig. 15) that winnowed away fine sediments leaving a coarse, armored substrate (Gelfenbaum et al., 2009; Warrick et al., 2011; Webster et al., 2013). Boulders of all sizes, which were remnants left from eroding glacial deposits, remained scattered on the seafloor. Rubin et al. (2011) characterized the pre-dam removal delta substrate, based on mapping by Cochran et al. (2008) and Warrick et al. (2008), as predominately gravel- and cobble-sized sediment, with areas of bedrock, boulders, and some sand. Rubin et al. (2011) classified the subaqueous delta into habitat types based on a series of SCUBA dive surveys to assess benthic habitat and biological communities. These substrate types, from sand to bedrock, were favorable for a variety of submerged aquatic vegetation (10 different species of kelp), invertebrates (65 different invertebrate taxa), and certain fish (24 different fish taxa).

During the dam removal process, turbid plumes were common and portions of the seafloor substrate changed relative to pre-dam removal conditions (Figs. 9 and 10). As sandy and muddy sediments deposited on the inner part of the subaqueous delta, large boulders that were sitting on the seafloor likely became buried and the seafloor lost some of its rugosity. These grain size and roughness changes in seafloor substrate are probably affecting habitat suitability. Initial results from dive surveys of habitat and biological use one and two years after dam removal show decreases in kelp density of 60–100% in the area adjacent to the river mouth compared to pre-dam removal (Steve Rubin, USGS, personal communication, 2014). The exact causes of the decrease in kelp density are uncertain, but may result from a decrease in light availability during the kelp's growing periods, a decrease in rocky or hard substrate for kelp to attach, scouring of kelp recruits by high suspended sediment loads, or a combination of all three. Even as kelp density is reduced, though, other species may benefit or not be affected at all by the rapid change in substrate (Thrush et al., 2004; Wheatcroft, 2006; Rubin et al., 2011). Continued monitoring of habitat and community response to increased sediment supply following Elwha River dam removal provides a unique opportunity to study the geological and the biological consequences of river restoration in the coastal environment.

6. Summary

Two dams built in the early 1900s on the Elwha River in the U.S. Pacific Northwest trapped ~20 million m³ of sediment, drastically reducing loads to the coast contributing to beach erosion and substrate coarsening around the Elwha River delta. Removal of the two dams on the Elwha River, which began in September 2011, has provided an opportunity to examine, at full scale and within a short time frame, the effects of changing sediment supply on delta morphology.

We measured the accumulation of sediment on the Elwha delta prior to the start of and within the first two years of dam removal by comparing detailed DEMs made from repeat surveys of beach topography and nearshore bathymetry. We calculated a sediment budget from volume changes in various portions of the delta and measured the changes in substrate sediments on the beaches and offshore. In order to help explain the measured patterns of sediment dispersal and accumulation, we used a process-based numerical model to simulate the hydrodynamics and sediment transport. In summary, we show that:

- Prior to dam removal, eastside beaches were eroding and other portions of the delta were relatively stable compared to the changes

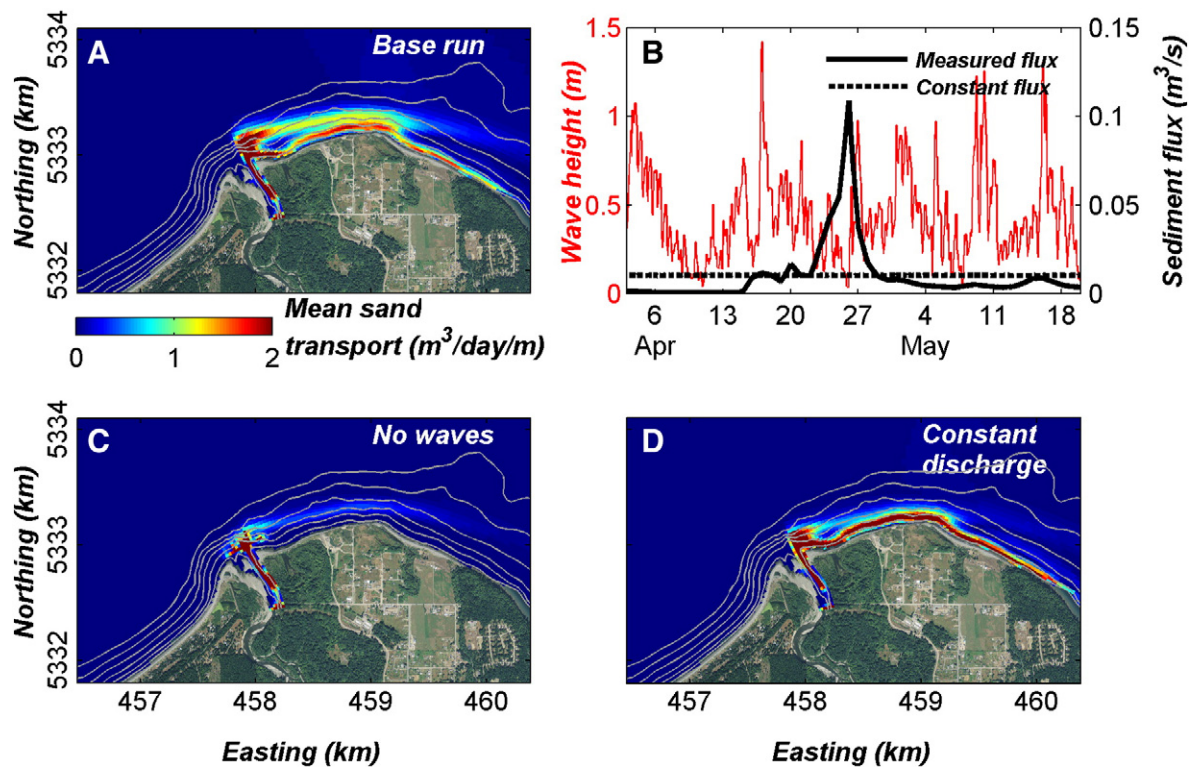


Fig. 17. Model simulations of sediment transport under several scenarios showing importance of waves (wave resuspension) and river discharge events (floods) on sediment dispersal. (A) Base case: waves increase suspended sediment concentrations enhancing tidally driven alongshore transport and flood events push region of sediment transport farther offshore. (B) Time series of waves and river discharge used in base case and constant discharge. (C) No waves result in less tidally driven sediment carried east. (D) Constant discharge results in sediment transport remaining closer to shore in shallow water.

that would occur after the dams were removed. Prior to dam removal, the inner delta was accumulating sediments slightly in some areas and eroding in others. Beaches on the east side of the subaerial delta were rapidly eroding up to tens of meters per year. During the first two years after the initiation of dam removal, 2.5 million m³ of sediment accumulated on the delta, about a 100-fold increase compared to pre-dam removal accumulation rates. Newly accumulated sediment caused the active depositional region of the delta to expand hundreds of meters seaward and nearly 1 km to the east. Close to the river mouth, the beaches prograded, but farther eastward the beaches continued to erode even though sediment was accumulating farther offshore.

- A sediment budget shows that during the first two years of dam removal approximately 6% of the fine sediment (silt and clay) and 70% of the coarse sediment (sand and gravel) transported down the river can be found in the coastal zone (beaches, active delta, and relict subaqueous delta).
- The coastal geomorphology of the active delta changed rapidly from a wave-dominated shape to a river-dominated shape as sediment supply to the coast increased after dam removal began. This transition may have been modulated by a seasonal change in wave characteristics over the delta. The active delta seems to respond quickly to changes in forcing and the river-dominated morphology observed at the end of the second year of dam removal is not necessarily the final equilibrium shape of the Elwha delta.
- The dominant processes of tides, waves, and river discharge were captured in a hydrodynamic and sediment transport model that successfully predicted the complex patterns of sediment dispersal and deposition. Together the model and in-situ field observations showed that large-scale transient eddies, formed as the tides traversed the delta, disperse fine sediments (silts and clays) west and east of the river mouth. Interaction of the submarine delta and the tides induce large residual eddies, offset eastward from the subaerial delta, that

drive a net eastward sand transport near the mouth of the river; and the secondary deposit, east of the main deposit, was formed where the large residual tidal eddies converged.

- Prior to dam removal, delta substrate was generally coarse and armored and the seafloor was rough, favoring specific fauna and flora including several kelp species. Sediment newly deposited on the inner delta derived from dam removal is finer and is changing substrate, habitats, and community structure on a portion of the delta. The majority of the larger submarine delta farther from the river mouth has been unchanged by the dam removal thus far.

Acknowledgments

This work was funded by the Coastal Habitats in Puget Sound (CHIPS) Project and the USGS's Coastal and Marine Geology Program. Additional funding was provided by an EPA grant to support monitoring impacts of ecosystem restoration in Puget Sound. Authors ASO and EFE were funded under NSF grant # OCE-0960788. We thank the members and staff of the Lower Elwha Klallam Tribe (LEKT) for support and access during this study. We thank Edwin Elias, Deltares, for help setting up the numerical model and George Kaminsky, Andrew Schwartz, Heather Baron, Diana McCandless, and the rest of the field crew from WA DOE for assisting in the mapping of the Elwha delta. We thank Karsten Turrey, LEKT, and Jacob Melly from the Huxley College on the Peninsulas for help analyzing grain size photos. We thank Steve Rubin, Nancy Elder, Reginald Reisenbichler, and the rest of the dive crew. We also thank David Finlayson, Pete dal Ferro, Jenny White, Joanne Thede-Ferreira, and the crew of the *R/V Parke Snavelly*. Finally we thank Jeff Duda, Jeff List, and an anonymous reviewer for their constructive comments of an earlier draft of this manuscript.

Appendix A. Supplementary data

Supplementary data to this article can be found online at <http://dx.doi.org/10.1016/j.geomorph.2015.01.002>.

References

- Allersma, E., 1988. Composition and density of sediments. Report Z71.03, Delft Hydraulics, Delft. Delft Hydraulics, The Netherlands.
- Barnard, P.L., Warrick, J.A., 2010. Dramatic beach and nearshore morphological changes due to extreme flooding at a wave-dominated river mouth. *Mar. Geol.* 271, 131–148.
- Booij, N., Ris, R.C., Holthuijsen, L.H., 1999. A third-generation wave model for coastal regions, 1, model description and validation. *J. Geophys. Res.* 104, 7649–7666.
- Bountry, J., Ferrari, R., Wille, K., Randle, T.J., 2010. 2010 survey report and area-capacity tables for Lake Mills and Lake Aldwell on the Elwha River, Washington. U.S. Department of Interior, Bureau of Reclamation Technical Report SRH-2010-23 (66 p.).
- Cochrane, G.R., Warrick, J.A., Sagy, Y., Finlayson, D., Harney, J., 2008. Sea-floor mapping and benthic habitat for the Elwha River delta nearshore, Washington. U.S. Geological Survey Data Series 320 (<http://pubs.usgs.gov/ds/320/>).
- Curran, C.A., Konrad, C.P., Higgins, J.L., Bryant, M.K., 2009. Estimates of sediment load prior to dam removal in the Elwha River, Clallam County, Washington. U.S. Geological Survey Scientific Investigations Report 2009-5221 (18 p.).
- Czuba, C.R., Randle, T.J., Bountry, J.A., Magirl, C.S., Czuba, J.A., Curran, C.A., Konrad, C.P., 2011. Anticipated sediment delivery to the lower Elwha River during and following dam removal. In: Duda, J.J., Warrick, J.A., Magirl, C.S. (Eds.), *Coastal Habitats of the Elwha River, Washington—Biological and Physical Patterns and Processes Prior to Dam Removal*. U.S. Geological Survey Scientific Investigations Report 2011-5120, pp. 27–46.
- Davis, J.C., 2002. *Statistics and Data Analysis in Geology*. Third ed. John Wiley & Sons, New York.
- Draut, A.E., Logan, J.B., Mastin, M.C., 2011. Channel evolution on the dammed Elwha River, Washington. *USA. Geomorphology* 127, 71–87.
- Duda, J.J., Warrick, J.A., Magirl, C.S., 2011. Coastal and lower Elwha River, Washington, prior to dam removal – history, status, and defining characteristics. In: Duda, J.J., Warrick, J.A., Magirl, C.S. (Eds.), *Coastal Habitats of the Elwha River, Washington—Biological and Physical Patterns and Processes Prior to Dam Removal*. U.S. Geological Survey Scientific Investigations Report 2011-5120, pp. 1–26.
- East, A.E., Pess, G.R., Bountry, J.A., Magirl, C.S., Ritchie, A.C., Logan, J.B., Randle, T.J., Mastin, M.C., Minear, J.T., Duda, J.J., Liermann, M.C., McHenry, M.L., Beechie, T.J., Shafroth, P.B., 2015. Large-scale dam removal on the Elwha River, Washington, USA: river channel and floodplain geomorphic change. *Geomorphology* 228, 765–786. <http://dx.doi.org/10.1016/j.geomorph.2014.08.028>.
- Eidam, E.F., Ogston, A.S., Nittrouer, C.A., Warrick, J.A., 2014. Sediment dispersal and deposition on a submarine delta during dam removal: Elwha River. *WA. Ocean Sciences 2014 Program*. Honolulu, HI (95 p.).
- Eidam, E.F., Ogston, A.S., Nittrouer, C.A., Warrick, J.A., 2015n. Tidally Dominated Sediment Dispersal Offshore of a Small Mountainous River (Elwha River, WA) (in preparation).
- Elias, E., Gelfenbaum, G., Van der Westhuisen, A., 2012. Validation of a coupled wave-flow model in a high-energy setting: the mouth of the Columbia River. *J. Geophys. Res. Oceans* 117, C09011.
- Fatorič, S., Chelleri, L., 2012. Vulnerability to the effects of climate change and adaptation: the case of the Spanish Ebro Delta. *Ocean Coast. Manage.* 60, 1–10.
- Finlayson, D.P., Miller, I.M., Warrick, J.A., 2011. Bathymetry and acoustic backscatter—Elwha River Delta, Washington: U.S. Geological Survey Open-file Report 2011-1226 (<http://pubs.usgs.gov/of/2011/1226/>).
- Foreman, M.G.G., Sutherland, G., Cummins, P.F., 2004. Tidal dissipation around Vancouver island: an inverse approach. *Cont. Shelf Res.* 24, 2167–2185.
- Galloway, W.E., 1975. Process framework for describing the morphologic and stratigraphic evolution of deltaic depositional systems. In: Broussard, M.L. (Ed.), *Deltas, Models for Exploration*. Houston Geological Society, Houston, TX, pp. 87–98.
- Galster, R.W., Schwartz, M.L., 1990. Ediz Hook – a case history of coastal erosion and rehabilitation. *J. Coast. Res.* 6, 103–113.
- Geleynse, N., Storms, J.E.A., Walstra, D.J.R., Jagers, H.R.A., Wang, Z.B., Stive, M.J.F., 2011. Controls on river delta formation; insights from numerical modeling. *Earth Planet. Sci. Lett.* 302, 217–226.
- Gelfenbaum, G., Kaminsky, G.M., 2010. Large-scale coastal change in the Columbia River littoral cell: an overview. *Mar. Geol.* 273, 1–10.
- Gelfenbaum, G., Stevens, A., Elias, E., Warrick, J., 2009. Modeling sediment transport and delta morphology on the dammed Elwha River, Washington State, USA. In: Mizuguchi, M., Sato, S. (Eds.), *Proceedings of Coastal Dynamics 2009: Impacts of Human Activities on Dynamic Coastal Processes*. World Scientific, Tokyo Japan.
- Gelfenbaum, G., Duda, J.J., Warrick, J.A., 2011. Summary and anticipated responses to Elwha River dam removal. In: Duda, J.J., Warrick, J.A., Magirl, C.S. (Eds.), *Coastal Habitats of the Elwha River, Washington—Biological and Physical Patterns and Processes Prior to Dam Removal*. U.S. Geological Survey Scientific Investigations Report 2011-5120, pp. 249–263.
- Geyer, W.R., Hill, P., Milligan, T., Traykovski, P., 2000. The structure of the Eel River plume during floods. *Cont. Shelf Res.* 20, 2067–2093.
- Gilbert, J.D., Link, R.A., 1995. Alluvium distribution in Lake Mills, Glines Canyon Project, and Lake Aldwell, Elwha Project, Washington. U.S. Department of Interior Elwha Technical Series PN-95-4 (60 p.).
- Goodbred, S.L., Kuehl, S.A., 1999. Holocene and modern sediment budgets for the Ganges–Brahmaputra River: Evidence for highstand dispersal to flood-plain, shelf, and deep-sea depocenters. *Geology* 27, 559–562.
- Hicks, D.M., Inman, D.L., 1987. Sand dispersion from an ephemeral delta on the Central California coast. *Mar. Geol.* 77, 305–318.
- Jimenez, J.A., Sanchez-Arcilla, A., 1993. Medium-term coastal response at the Ebro delta, Spain. *Mar. Geol.* 114, 105–118.
- Kaminsky, G.M., Ruggiero, P., Buijsman, M., McCandless, D., Gelfenbaum, G., 2010. Historical evolution of the Columbia River littoral cell. *Mar. Geol.* 273, 96–126.
- Kuenzi, D.W., Horst, O.H., McGehee, R.V., 1979. Effect of volcanic activity on fluvial–deltaic sedimentation in a modern arc–trench gap, southwestern Guatemala. *Geol. Soc. Am. Bull.* 90, 827–838.
- Law, B.A., Hill, P.S., Milligan, T.G., Curran, K.J., Wiberg, P.L., Wheatcroft, R.A., 2007. Size sorting of fine-grained sediments during erosion: results from the western Gulf of Lions. *Cont. Shelf Res.* 28, 1935–1946.
- Lesser, G.R., Roelvink, J.A., van Kester, J.A.T.M., Stelling, G.S., 2004. Development and validation of a three-dimensional morphological model. *Coast. Eng.* 51, 883–915.
- Magirl, C.S., Curran, C.A., Sheibley, R.W., Warrick, J.A., Czuba, J.A., Czuba, C.R., Gendaszek, A.S., Shafroth, P.B., Duda, J.J., Foreman, J.R., 2011. Baseline hydrologic studies in the lower Elwha River prior to dam removal. In: Duda, J.J., Warrick, J.A., Magirl, C.S. (Eds.), *Coastal Habitats of the Elwha River, Washington—Biological and Physical Patterns and Processes Prior to Dam Removal*. U.S. Geological Survey Scientific Investigations Report 2011-5120, pp. 75–110.
- Magirl, C.S., Hilldale, R.C., Curran, C.A., Duda, J.J., Straub, T.D., Domanski, M., Foreman, J.R., 2015. Large-scale dam removal on the Elwha River, Washington, USA: fluvial sediment load. *Geomorphology* 246, 669–686.
- Miller, I.M., Warrick, J.A., 2012. Measuring sediment transport and bed disturbance with tracers on a mixed beach. *Mar. Geol.* 299–302, 1–17.
- Miller, I.M., Warrick, J.A., Morgan, C., 2011. Observations of coarse sediment movements on the mixed beach of the Elwha Delta, Washington. *Mar. Geol.* 282, 201–214.
- Orton, G.J., Reading, H.G., 1993. Variability of deltaic processes in terms of sediment supply, with particular emphasis on grain size. *Sedimentology* 40 (3), 475–512.
- Randle, T.J., Bountry, J.A., Ritchie, A.C., Wille, K.B., 2015. Large-scale dam removal on the Elwha River, Washington, USA: erosion of reservoir sediment. *Geomorphology* 246, 709–728.
- Rubin, S.P., Miller, I.M., Elder, N., Reisenbichler, R.R., Duda, J.J., 2011. Nearshore biological communities prior to removal of the Elwha River dams. In: Duda, J.J., Warrick, J.A., Magirl, C.S. (Eds.), *Coastal Habitats of the Elwha River, Washington—Biological and Physical Patterns and Processes Prior to Dam Removal*. U.S. Geological Survey Scientific Investigations Report 2011-5120, pp. 131–174.
- Ruggiero, P., Kaminsky, G.A., Gelfenbaum, G., Voigt, B., 2005. Seasonal to interannual morphodynamics along a high-energy dissipative littoral cell. *J. Coast. Res.* 21, 553–578.
- Sallenger, A.H., Krabill, W.B., Swift, R.N., Brock, J., List, J., Hansen, M., Holman, R.A., Manizade, S., Sontag, J., Meredith, A., Morgan, K., Yunkel, J.K., Frederick, E.B., Stockdon, H., 2003. Evaluation of airborne topographic lidar for quantifying beach changes. *J. Coast. Res.* 19, 125–133.
- Sanchez-Arcilla, A., Jimenez, J.A., Valdemoro, H.L., 1998. The Ebro Delta: morphodynamics and vulnerability. *J. Coast. Res.* 14, 754–772.
- Signell, R.P., Geyer, W.R., 1991. Transient eddy formation around headlands. *J. Geophys. Res.* 96, 2561–2576.
- Smith, S.E., Abdel-Kader, A., 1988. Coastal erosion along the Egyptian Delta. *J. Coast. Res.* 4, 245–255.
- Soulsby, R.L., Hamm, L., Klopman, G., Myrhaug, D., Simons, R.R., Thomas, G.P., 1993. Wave-current interaction within and outside the bottom boundary layer. *Coast. Eng.* 21, 41–67.
- Stumpf, R.P., Gelfenbaum, G., Pennock, J.R., 1993. Wind and tidal forcing of a buoyant plume: Mobile Bay, Alabama. *Cont. Shelf Res.* 13, 1281–1301.
- Sutherland, D.A., MacCready, P., Banas, N.S., Smedstad, L.F., 2011. A model study of the Salsish Sea estuarine circulation. *J. Phys. Oceanogr.* 41, 1125–1143.
- Thrush, S.F., Hewitt, J.E., Cummings, V.J., Ellis, J.A., Hutton, C., Lohrer, A., Norkko, A., 2004. Muddy waters: elevating sediment input to coastal and estuarine habitats. *Front. Ecol. Environ.* 2, 299–306.
- van Rijn, L.C., 2005. *Principles of Sediment Transport in Rivers, Estuaries, and Coastal Seas*. Aqua Publications, Amsterdam, The Netherlands.
- Walstra, D.J.R., Roelvink, J.A., Groeneweg, J., 2000. Calculation of wave-driven currents in a 3D mean flow model. *Proceedings of the 27th International Conference on Coastal Engineering*. ASCE, Sydney, Australia.
- Warrick, J.A., Stevens, A.W., 2011. A buoyant plume adjacent to a headland—observations of the Elwha River plume. *Cont. Shelf Res.* 31, 85–97.
- Warrick, J.A., Cochrane, G.R., Sagy, Y., Gelfenbaum, G., 2008. Nearshore substrate and morphology offshore of the Elwha River, Washington. *Northwest Sci.* 82, 153–163.
- Warrick, J.A., George, D.A., Gelfenbaum, G., Ruggiero, P., Kaminsky, G.M., Beirne, M., 2009a. Beach morphology and change along the mixed grain-size delta of the dammed Elwha River, Washington. *Geomorphology* 111, 136–148.
- Warrick, J.A., Rubin, D.M., Ruggiero, P., Harney, J.N., Draut, A.E., Buscombe, D., 2009b. Cobble cam: grain-size measurements of sand to boulder from digital photographs and autocorrelation analyses. *Earth Surf. Process. Landf.* 34, 1811–1821.
- Warrick, J.A., Stevens, A.W., Miller, I.M., Gelfenbaum, G., 2011. Coastal processes of the Elwha River Delta. In: Duda, J.J., Warrick, J.A., Magirl, C.S. (Eds.), *Coastal Habitats of the Elwha River, Washington—Biological and Physical Patterns and Processes Prior to Dam Removal*. U.S. Geological Survey Scientific Investigations Report 2011-5120, pp. 111–130.
- Warrick, J.A., Duda, J.J., Magirl, C.S., Curran, C.A., 2012. River turbidity and sediment loads during dam removal. *Trans. Am. Geophys. Union* 93, 425–426.
- Warrick, J.A., Bountry, J.A., East, A.E., Magirl, C.S., Randle, T.J., Gelfenbaum, G., Ritchie, A.C., Pess, G.R., Leung, V., Duda, J.J., 2015. Large-scale dam removal on the Elwha River, Washington, USA: source-to-sink sediment budget and synthesis. *Geomorphology* 246, 729–750.

- Webster, K.L., Ogston, A.S., Nittrouer, C.A., 2013. Delivery, reworking and export of fine-grained sediment across the sandy Skagit River tidal flats. *Cont. Shelf Res.* 60, S58–S70.
- Wheatcroft, R.A., 2006. Time-series measurements of microbenthos abundance and sediment bioturbation intensity on a flood-dominated shelf. *Prog. Oceanogr.* 71, 88–122.
- Wheatcroft, R.A., Sommerfield, C.K., Drake, D.E., Borgeld, J.C., Nittrouer, C.A., 1997. Rapid and widespread dispersal of flood sediment on the northern California margin. *Geology* 25, 163–166.
- Wilcox, A.C., O'Connor, J.E., Major, J.J., 2014. Rapid reservoir erosion, hyperconcentrated flow, and downstream deposition triggered by breaching of 38-m tall Condit Dam, White Salmon River, Washington. *J. Geophys. Res. Earth Surf.* 119, 1376–1394.
- Willis, C.M., Griggs, G.B., 2003. Reductions in fluvial sediment discharge by coastal dams in California and implications for beach sustainability. *J. Geol.* 111, 167–182.
- Willmott, C.J., 1982. Some comments on the evaluation of model performance. *Bull. Am. Meteorol. Soc.* 63, 1309–1313.
- Wright, L.D., 1977. Sediment transport and deposition at river mouths: a synthesis. *Geol. Soc. Am. Bull.* 88, 857–868.
- Wright, L.D., Coleman, J.M., 1973. Variations in morphology of major river deltas as functions of ocean wave and river discharge regimes. *Am. Assoc. Pet. Geol. Bull.* 57, 370–398.
- Wright, L.D., Short, A.D., 1984. Morphodynamic variability of surf zones and beaches: a synthesis. *Mar. Geol.* 56, 93–118.